UNIVERSIDADE FEDERAL DO RIO GRANDE DO SUL
INSTITUTO DE CIÊNCIAS BÁSICAS DA SAÚDE
PROGRAMA DE PÓS-GRADUAÇÃO EM CIÊNCIAS BIOLÓGICAS: FISIOLOGIA

GABRIEL FRANCISCO POZO DE MATTOS PEREIRA

# DISSECANDO A COMPOSIÇÃO E AS INTERAÇÕES CELULARES DO MICROAMBIENTE TUMORAL NA PROGRESSÃO DO ADENOCARCINOMA DUCTAL PANCREÁTICO

Porto Alegre
2022

GABRIEL FRANCISCO POZO DE MATTOS PEREIRA

# DISSECANDO A COMPOSIÇÃO E AS INTERAÇÕES CELULARES DO MICROAMBIENTE TUMORAL NA PROGRESSÃO DO ADENOCARCINOMA DUCTAL PANCREÁTICO

Dissertação apresentada ao Programa de Pós-Graduação em Ciências Biológicas: Fisiologia do Instituto de Ciências Básicas da Saúde da Universidade Federal do Rio Grande do Sul como requisito parcial para a obtenção do título de mestre(a) em Fisiologia.

Orientador: Prof. Dr. Eduardo Cremonese Filippi-Chiela

Porto Alegre

2022

CIP - Catalogação na Publicação

Pozo de Mattos Pereira, Gabriel Francisco
DISSECANDO A COMPOSIÇÃO E AS INTERAÇÕES CELULARES DO MICROAMBIENTE TUMORAL NA PROGRESSÃO DO ADENOCARCINOMA DUCTAL PANCREÁTICO / Gabriel Francisco Pozo de Mattos Pereira. -- 2022.
80 f.
Orientador: Eduardo Cremonese Fillipi-Chiela.

Dissertação (Mestrado) -- Universidade Federal do Rio Grande do Sul, Instituto de Ciências Básicas da Saúde, Programa de Pós-Graduação em Ciências Biológicas: Fisiologia, Porto Alegre, BR-RS, 2022.

1. Câncer de pâncreas. 2. Microambiente tumoral. 3. Sequenciamento de células únicas. 4. Composição celular. I. Cremonese Fillipi-Chiela, Eduardo, orient. II. Título.

Elaborada pelo Sistema de Geração Automática de Ficha Catalográfica da UFRGS com os dados fornecidos pelo(a) autor(a).

## AGRADECIMENTOS

Agradeço aos meus pais, Marília Pozo de Mattos e Fábio André Pereira, por todo amor, apoio e incentivo, especialmente por estarem sempre dispostos a ouvir sobre minhas hipóteses sobre câncer e microambiente tumoral ao longo desse período. Aos meus amigos pelos momentos de descontração, companheirismo e apoio.

Agradecimento em especial ao meu orientador, professor Dr. Eduardo Chiela, por toda dedicação, parceria, confiança e inúmeros aprendizados desde a especialização até o presente momento. O caminho só foi menos difícil graças a ti. Ao professor Dr. Alessandro Osvaldt pela confiança, incentivo e pela oportunidade de acompanhar a equipe do CAD, Cirurgia do Aparelho Digestivo, do Hospital de Clínicas de Porto Alegre. Uma oportunidade que agregou bastante na minha formação acadêmica, mas também no desenvolvimento pessoal. A Drª. Simone Machado pela disposição e pelos ensinamentos de patologia. Agradeço aos colegas do grupo LaBCM e do grupo do Pâncreas pelas críticas construtivas e discussões científicas que impactaram positivamente neste trabalho.

Por último, gostaria de agradecer ao meu avô, Ruy Amaro de Mattos, que nos deixou há mais de 5 anos, porém todo ensinamento, apoio, incentivo, amor e carinho ficarão para sempre.

“You, me, or nobody is gonna hit as hard as life. But it ain't about how hard you hit. It's about how hard you can get hit and keep moving forward. How much you can take and keep moving forward.” (Rocky Balboa)

## RESUMO

O adenocarcinoma ductal pancreático (ADP) é uma doença mortal bem conhecida por seu microambiente tumoral heterogêneo. O sequenciamento de RNA de células individuais (scRNA-seq) tem sido amplamente utilizado para caracterizar a heterogeneidade intratumoral e intertumoral do ADP. No entanto, a dinâmica da composição celular do microambiente tumoral e a comunicação intercelular durante a progressão do ADP não são totalmente compreendidas. Aqui, integramos dados de scRNA-seq de quatro coortes diferentes contendo quatro locais de tecidos distintos. Observamos uma proporção maior de células T CD8 de memória em amostras de tecido adjacente do que em amostras malignas. Por outro lado, células T reguladoras e células T CD8 disfuncionais ($GZMK^+$ CD8) estavam entre os tipos celulares mais prevalentes nas amostras malignas. Os macrófagos foram o tipo de célula mais abundante no componente mielóide. Identificamos quatro grupos de macrófagos; A análise de pseudotime sugeriu uma origem comum para os macrófagos $C1Q^+$ e $SPP1^+$. Como esperado, os CAFs (fibroblastos associados ao tumor) estavam enriquecidos no ADP. A análise de trajetória para células estromais revelou uma transição de células estreladas para miofibroblastos associados ao tumor (myCAF). Após a anotação refinada dos tipos celulares, construímos uma rede de interações célula-célula que desvendou os CAFs como a principal fonte de sinais extracelulares. Em contrapartida, as células T CD8 foram o destino final mais frequente para múltiplos sinais no microambiente tumoral. Nossos resultados fornecem uma caracterização refinada da composição celular e dinâmica de interação célula-célula para o microambiente do ADP.



**Palavras-chave:** sequenciamento de células únicas, adenocarcinoma ductal pancreático, microambiente tumoral, comunicação intercelular, composição cellular

## ABSTRACT

Pancreatic ductal adenocarcinoma (PDAC) is a deadly disease well known for its heterogeneous tumor microenvironment (TME). Single-cell RNA sequencing (scRNA-seq) has been extensevily used to characterize the intratumor and intertumor heterogeneity of PDAC. However, TME cellular composition dynamics and intercellular communication during PDAC's progression are not fully comprehended. Here, we integrated scRNA-seq data from four different datasets containing four distinct tissue sites. We observed a higher proportion of memory CD8 T cells in adjacent tissue samples than malignant samples. On the other hand, regulatory T cells and dysfunctional CD8 T cells ($GZMK^+$ CD8) were among the most prevalent cell type in malignant samples. Macrophages were the most abundant cell type in the myeloid component. We identified four clusters of macrophages; pseudotime analysis suggested a potential common origin for $C1Q^+$ Macro and $SPP1^+$ Macro. As expected, CAFs (cancer-associated fibroblasts) were enriched in PDAC. Trajectory analysis for stromal cells revealed a transition from stellate cells to myofibroblastic CAFs (myCAF). After refined cell type annotation, we built cell-cell interactions network that unraveled CAFs as the major source of extracellular signals. In contrast, CD8 T cells were the most frequent final destination for multiple signals in the TME. Our results provide a refined characterization of cell composition and cell-cell interaction dynamics for PDAC microenvironment.



**Keywords:** single-cell sequencing, pancreatic ductal adenocarcinoma, tumor microenvironment, intercellular communication, cell composition

## LISTA DE FIGURAS

**Figura 1 - Modelo da progressão tumoral do ADP e principais genes alterados** ..... 11

**Figura 2 - O complexo ecossistema de um microambiente tumoral** ..... 12

**Figura 3 – Os três subtipos histológicos de submicroambientes tumorais no ADP** ..... 14

,

## LISTA DE ABREVIATURAS

AdjTumor - tecido adjacente

ADP - adenocarcinoma ductal pancreático

apCAF - fibroblastos apresentadores de antígeno associados ao tumor

CAF - fibroblastos associados ao tumor

cDC1 - células dendríticas convencionais do tipo I

cDC2 - células dendríticas convencionais do tipo II

DC - células dendríticas

ECM - matriz extracelular

EMT - transição epitélio mesênquima

iCAF - fibroblastos inflamatórios associados ao tumor

IPMN - neoplasia mucinosa papilar intraductal

L-R - ligante-receptor

MAIT - células T invariantes de mucosa

MET - tecido metastático

MHC - complexo de histocompatibilidade principal

myCAF - miofibroblastos associados ao tumor

NK - células natural killer

PanIN - neoplasia intraepitelial pancreática

PDAC - adenocarcinoma ductal pancreático

scRNA-seq - sequenciamento de RNA de células únicas

SHH - sonic hedgehog

TME - microambiente tumoral

Treg - células T reguladoras

**SUMÁRIO**

1. INTRODUÇÃO.....10
1.1 O adenocarcinoma ductal pancreático (ADP).....10
1.2 O microambiente tumoral.....12
1.3 O microambiente tumoral do ADP.....13
1.3.1 Os fibroblastos associados ao tumor (CAFs).....15
1.3.2 O estroma do ADP: células e matriz extracelular (composição e organização).....17
1.3.3 Os componentes linfoide e mieloide no ADP.....17
1.4 As lesões precursoras do ADP e seus respectivos microambientes.....19
2. JUSTIFICATIVA.....20
3. QUESTÃO DE PESQUISA.....21
4. HIPÓTESE.....22
5. OBJETIVOS.....23
5.1 OBJETIVO GERAL.....23
5.2 OBJETIVOS ESPECÍFICOS.....23
6. ARTIGO CIENTÍFICO.....24
7. CONCLUSÕES E PERSPECTIVAS.....70
REFERÊNCIAS.....72

# 1. INTRODUÇÃO

## 1.1. O Adenocarcinoma Ductal Pancreático (ADP)

O adenocarcinoma ductal pancreático (ADP) é um tumor de origem exócrina e representa 90% das neoplasias pancreáticas. Em 2020, foram registrados 495,733 casos e 466,003 mortes por ADP no mundo (GLOBOCAN, 2020). A incidência vem aumentando mundialmente, e estima-se que até 2030, o ADP seja a segunda neoplasia mais letal nos Estados Unidos (Rahib et al., 2014).

Um dos aspectos que mais chamam a atenção desta neoplasia é a agressividade. A maioria dos pacientes já apresenta lesões metastáticas no momento do diagnóstico e cerca de 35% apresentam doença localmente avançada (Kleeff et al., 2016). O diagnóstico tardio impede que os pacientes sejam submetidos à ressecção cirúrgica, viável em apenas 15% dos casos (Park et al., 2021). A ausência de biomarcadores e sintomas específicos impede a triagem eficaz para o diagnóstico precoce. Somado a isso, cerca de 80% dos pacientes sofrerão com recidiva da doença após a ressecção (Luu et al., 2021). Todo este contexto faz com que a taxa de sobrevida em 5 anos seja inferior a 10% mesmo com o emprego de estratégias terapêuticas múltiplas (Siegel et al., 2021).

A ressecção cirúrgica é a única terapia curativa até o momento. Porém, devido à complexidade da doença e da anatomia do pâncreas, uma pequena parcela dos pacientes beneficiam-se. Usualmente, após a ressecção cirúrgica os pacientes são submetidos à quimioterapia adjuvante. Dentre os principais quimioterápicos majoritariamente utilizados na clínica temos o *cocktail* FOLFIRINOX (fluoracil, oxaliplatina, irinotecano e leucovorina). Além destes, gemcitabina, pactilaxel e capecitabina também aparecem como quimioterápicos de escolha para terapia do ADP (Regine et al., 2008). Os pacientes com doença borderline ou localmente avançada realizam quimioterapia neoadjuvante e conforme a resposta ao tratamento podem ser submetidos à ressecção. Os benefícios da quimioterapia neoadjuvante ainda estão sendo avaliados; no entanto, em um estudo clínico de fase 2, observou-se uma baixa resposta na maioria dos pacientes (Sohal et al., 2021).

Considerando a patogênese molecular, são conhecidos 4 genes drivers na carcinogênese do ADP: *KRAS*, *TP53*, *CDKN2A* e *SMAD4* (**Figura 1**). As vias de sinalização controladas por estes genes modulam desde proliferação e sobrevivência celular (*KRAS* e *CDKN2A*), passando por reparo de DNA e apoptose (*TP53*), até migração celular e transição epitélio-mesênquima

(*SMAD4*) (Hayashi et al., 2021). Estudos recentes apontam outros eventos genômicos relevantes para progressão tumoral incluindo aberrações cromossômicas como a cromotripsia, amplificação de *KRAS*, *MYC*, amplificação ou deleção de *GATA6* e até mesmo duplicação do genoma (Notta et al., 2016; Hayashi et al., 2020; Chan-Seng-Yue et al., 2020).

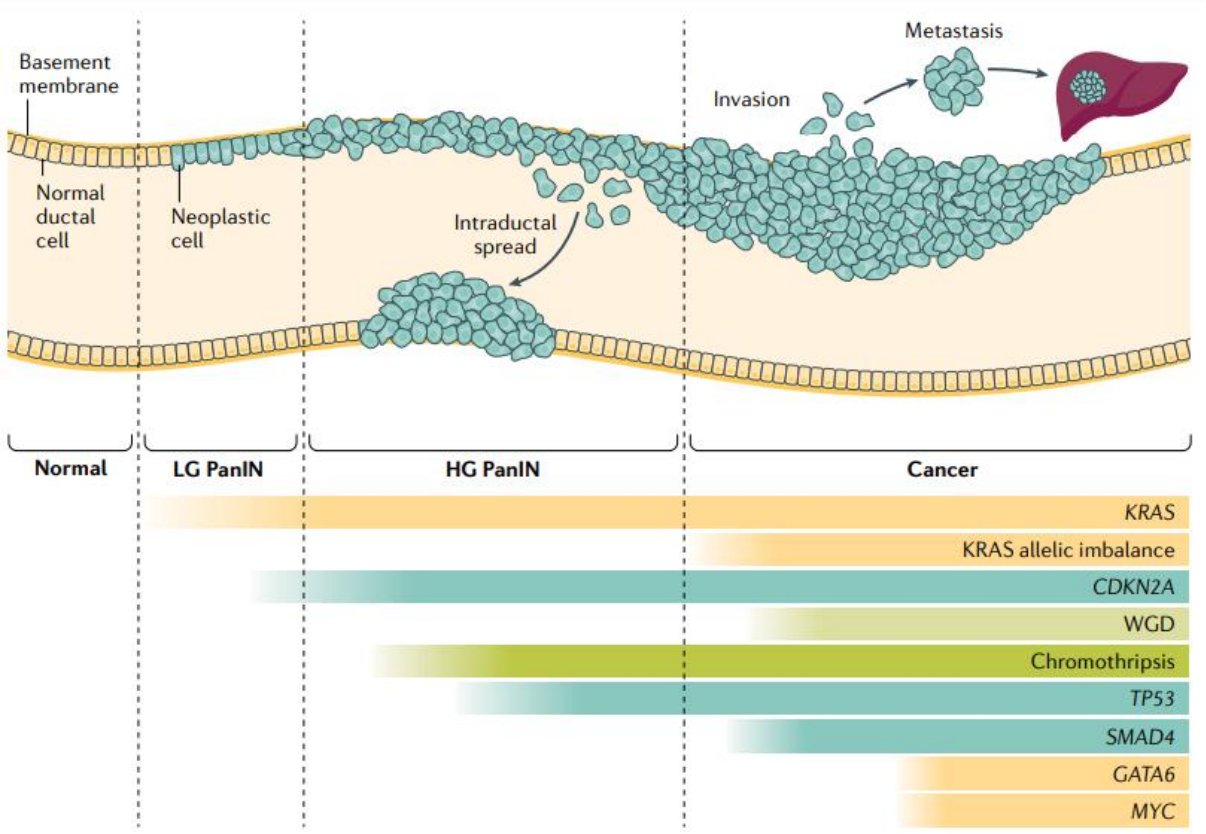



**Figura 1 - Modelo da progressão tumoral do ADP e principais genes alterados.** A partir do tecido epitelial normal, células neoplásicas podem originar lesões precursoras (PanIN – Pancreatic Intraepithelial Neoplasms), de baixo (LG) ou alto grau (HG). Nas PanINs de baixo grau já se observam alterações moleculares em genes driver como KRAS e CDKN2A. Porém, é a partir das lesões de alto grau que a incidência de alterações moleculares é mais pronunciada. Já nas neoplasias malignas, alterações em outros oncogenes e genes supressores tumorais envolvidos especialmente com migração celular e transição epitélio-mesênquima são observadas e favorecem a progressão tumoral. Fonte: Hayashi et al., 2021.

### 1.2 - O microambiente tumoral

O desenvolvimento e a manutenção de um câncer reside sobre 2 pilares da biologia: evolução e ecologia. Durante a progressão tumoral, observamos a seleção de clones e a formação de um ecossistema complexo resultado da interação entre as células tumorais e o microambiente tumoral (do inglês *tumor microenvironment*, ou TME) (**Figura 2 - Adaptada de Ushijima et al., 2021**). Esse ecossistema complexo é formado por células estromais, células imunes e células tumorais, além de componentes da matriz extracelular (MEC) (Haeberle L & Esposito I, 2019; Dougan K, 2019).

A distribuição espacial do microambiente não é randômica; podemos encontrar diferentes níveis (nichos) de organização desempenhando funções distintas ou até mutuamente exclusivas (Grünwald et al., 2021). As células não tumorais estabelecem interações intercelulares heterotípicas entre elas e com células malignas. Em modelos animais do ADP, a composição do TME é dinâmica ao longo da carcinogênese, desde lesões pré-malignas até o carcinoma invasivo (Hosein et al., 2019; Schlesinger et al., 2020). Além disso, a composição e a organização espacial do TME pode fornecer informações valiosas sobre a progressão do tumor, resposta à terapia e até mesmo prognóstico (Grünwald et al., 2021; Raghavan et al., 2021; Wang et al., 2021; Wu et al., 2021; Bagaev et al., 2021; Luca et al., 2021; Storrs et al., 2022).

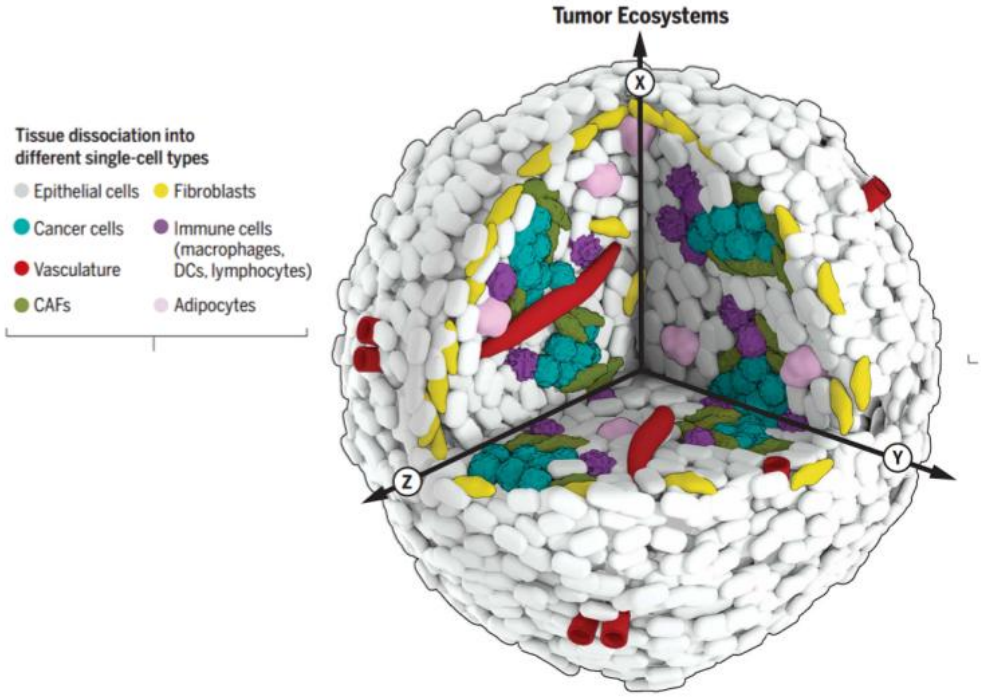


**Figura 2 - O complexo ecossistema de um microambiente tumoral.** Tumores são massas multicelulares compostas por células tumorais (usualmente conhecidas como ‘parênquima tumoral’), células do sistema imunológico (leucócitos granulócitos e agranulócitos), células estromais (fibroblastos, células endoteliais, células mesenquimais, adipócitos, entre outras), moléculas solúveis e matriz extracelular. Fonte: Ushijima et al., 2021.

### 1.3 - O microambiente tumoral do ADP

Uma das principais características do ADP é um microambiente fibrótico e imunossupressor, o qual é um dos grandes responsáveis pela agressividade dos tumores e ineficácia terapêutica (Ho et al., 2020). O ADP apresenta baixa heterogeneidade intratumoral de *drivers* observado pela grande semelhança encontrada entre lesões primárias e metastáticas do mesmo indivíduo (Makohon-Moore et al., 2017). Entretanto, já foram identificados pelo menos 3 subtipos moleculares baseados no perfil transcriptômico (clássico, intermediário e basal) e até mesmo células co-expressando 2 subtipos (clássico e basal) (Raghavan et al., 2021).

Então, de onde surge essa heterogeneidade do parênquima tumoral no ADP? Diversos estudos apontam o microambiente tumoral como o grande responsável pela plasticidade das células malignas. Chan-Seng-Yue e colaboradores observaram que eventos genômicos, como amplificação do oncogene *KRAS*, definiam o subtipo basal, o qual possui pior prognóstico (Chan-Seng-Yue et al., 2020). Contudo, um trabalho recente comparou lesões metastáticas primárias e organóides oriundos das respectivas lesões e, o subtipo tumoral sofria modificações: organóides de lesões primárias com subtipo basal adquiriram o perfil clássico devido à ausência de fatores secretados pelo microambiente. Adição desses fatores na cultura dos organóides foi capaz de recuperar o subtipo basal, sugerindo um papel primário do microambiente na determinação do perfil fenotípico tumoral (Raghavan et al., 2021).

A histologia do ADP é conhecida pela proliferação de células ductais com formação de estruturas normalmente chamadas de ‘glândulas tumorais’, dispersas em um estroma fibroso. Essa interação parênquima-estroma confere maior plasticidade fenotípica às células malignas tanto *in vitro*, em co-cultura de fibroblastos com células malignas, quanto nos pacientes. O aumento da plasticidade das glândulas tumorais apresentou correlação negativa com a sobrevida (Ligorio et al., 2019). Neste cenário, os fibroblastos são um dos principais personagens e desempenham funções relacionadas à remodelagem da matriz extracelular, inflamação, estabelecimento de um estado imunossupressor, resistência à quimio e

imunoterapia e até mesmo modulação da heterogeneidade intratumoral (Hessman et al., 2018; Wei et al., 2018; Dominguez et al., 2020; Su et al., 2018; Costa et al., 2018; Ligorio et al., 2019; Sahai et al., 2020).

Recentemente, foram descritos 3 subtipos de microambiente (a nível histológico) quanto à organização e prevalência de células ou matriz extracelular. Estes 3 subtipos apresentam funcionalidades distintas: a) subtipo desértico: caracterizado por escassez celular, alta deposição de colágeno e remodelagem da matriz extracelular; b) subtipo reativo: marcado por uma alta infiltração e diversidade celular; c) subtipo intermediário: representa um estado de transição entre os dois extremos (**Figura 3 - Adaptada de Grünwald et al., 2021**). Essa heterogeneidade não ocorre apenas entre os pacientes, mas também no mesmo paciente. A co-ocorrência de mais de um subtipo está associada a uma pior sobrevida. Os subtipos reativo e desértico exibiram correlação à progressão tumoral e resistência ao tratamento respectivamente. Após exposição à quimioterapia, observamos mudanças nos subtipos de microambiente com uma forte tendência do subtipo reativo tornar-se intermediário, intermediário virando desértico ou até mesmo a transição direta de reativo para desértico (Grünwald et al., 2021).

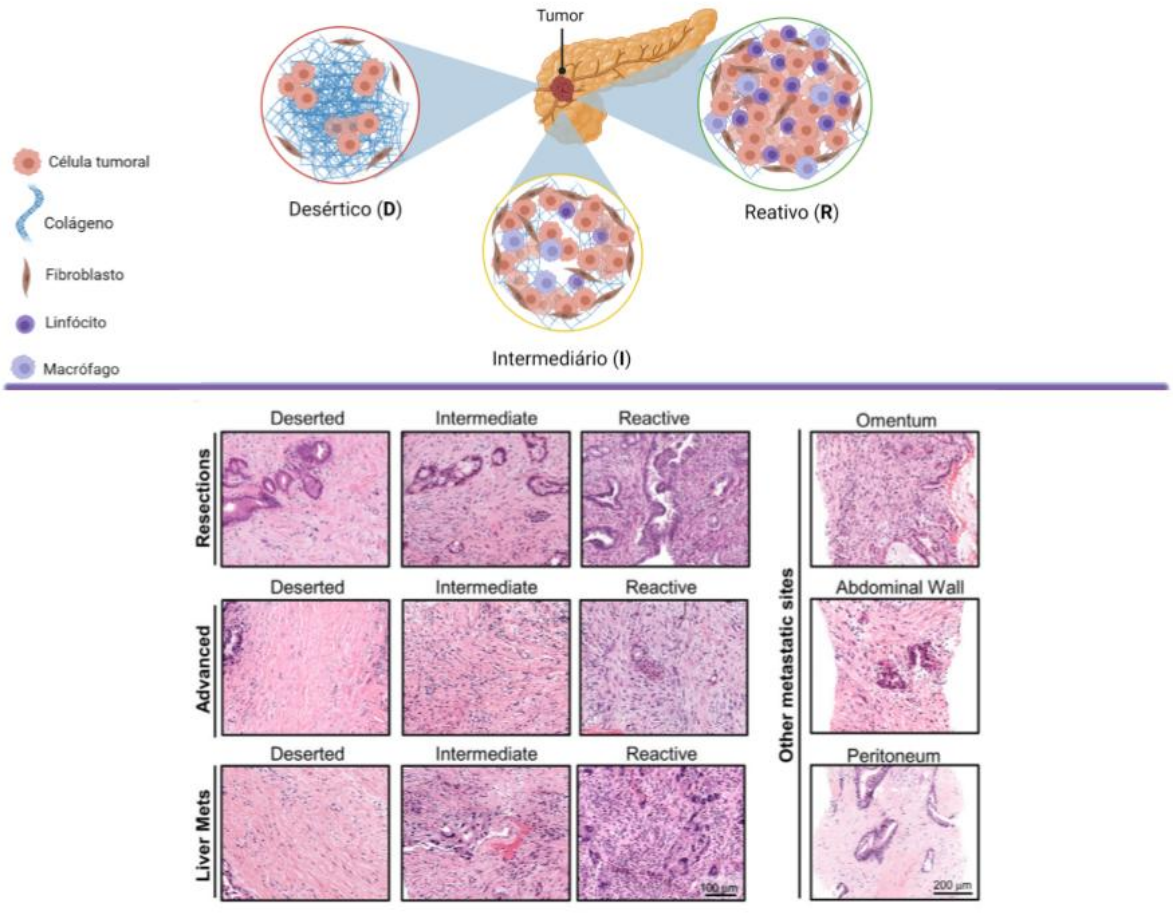


**Figura 3 – Os três subtipos histológicos de submicroambientes tumorais no ADP.** A organização e prevalência de células ou matriz extracelular tem sido utilizados para caracterização do microambiente tumoral. Acima, são mostrados esquemas representativos dos 3 subtipos (desértico, intermediário e reativo). Abaixo são mostradas imagens representativas de amostras primária coradas com hematoxilina e eosina, obtidas de ressecções cirúrgicas, tumores avançados e metástases. Adaptado de Grünwald et al., 2021.

Nas próximas seções, alguns detalhes relevantes dos principais tipos de células não-tumorais que compõem o microambiente tumoral são descritos.

### 1.3.1 - Fibroblastos associados ao tumor (CAFs)

Até o presente momento, já foram identificadas 3 subpopulações de CAFs: miofibroblastos associados ao tumor (myCAF), conhecidos pela alta expressão de αSMA+ (*ACTA2*); fibroblastos inflamatórios (iCAF), caracterizados pela expressão de citocinas com perfil inflamatório e imunossupressor (*CXCL12*, *LIF*, *IL11*, *IL6*); fibroblastos apresentadores de antígeno (apCAF), marcados pela expressão CD74 e HLA-DR em sua superfície (Elyada et al., 2019; Zhou et al., 2022). A distribuição espacial é importante para compreensão das interações celulares decorrentes no microambiente tumoral. Estas subpopulações de CAFs apresentam diferentes disposições espaciais e relacionam-se com suas respectivas funções (Öhlund et al., 2017; Ogawa et al., 2021). myCAF são encontrados próximos aos ductos tumorais realizando contato com as células tumorais, enquanto os iCAF e apCAF localizam-se mais distantes interagindo de forma parácrina e contato célula-célula, respectivamente, com o microambiente.

Molecularmente, as vias de sinalização celular que determinam a polarização das subpopulações de CAFs são Sonic Hedgehog (SHH), NF-kB, TGF-β e JAK/STAT (Garg et al., 2018; Biffi et al., 2019; Steele et al., 2021). O bloqueio da via de TGF-β reduz a expressão dos marcadores de myCAF e aumenta a expressão de marcadores iCAF direcionando os fibroblastos para um fenótipo imunossupressor (Biffi et al., 2019). Esse mesmo efeito é observado quando administrado um inibidor da via de SHH (Steele et al., 2021). Talvez essa seja uma das razões dos inibidores de SHH terem falhado na clínica, porque a polarização para iCAF promove infiltração de macrófagos M2, linfócitos Treg e reduz ativação dos linfócitos T $CD8^+$. Outra razão seria o impacto da via SHH em outras células do microambiente tumoral

como os linfócitos (Crompton et al., 2007; de La Roche et al., 2013). Já a inibição das vias JAK/STAT e NF-kB provoca a polarização dos fibroblastos no sentido inverso, de iCAF para myCAF. apCAF foram descritos no ADP com um papel imunorregulador através da interação com as células T $CD4^+$, pois devido a ausência de moléculas co-estimulatórias (CD28, CD40, CD80, CD86) são incapazes de promover ativação dos linfócitos e induzem anergia dos mesmos (Elyada et al., 2019; Biffi et al., 2019; Steele et al., 2021).

Os papeis da reação desmoplásica e dos myCAF ainda são controversos e sugerem um possível papel anti-tumoral. Em um estudo com modelo animal, a depleção dos myCAFs resultou em tumores pouco diferenciados, aceleração da progressão tumoral e uma grande infiltração de linfócitos Treg diminuindo a sobrevida dos animais (Özdemir et al., 2014). Um estudo recente publicado pelo mesmo grupo validou esses resultados a nível de *single-cell* após a deleção do gene *COL1A1* nos myCAF. Não houve alteração na composição dos CAFs, mas sim um aumento significativo de células mielóides imaturas com perfil imunossupressor levando à diminuição da sobrevida (Chen et al., 2021). Entretanto, uma análise *single-cell* de amostras humanas revelou a presença de um cluster de myCAF $LRRC15^+$ capaz de determinar a resposta à imunoterapia em diferentes neoplasias incluindo o ADP (Dominguez et al., 2020).

Apesar do relativo entendimento de algumas vias que poderiam participam da definição dos diferentes fenótipos de CAFs, a origem dessas células no microambiente tumoral segue incerta. De fato, CAFs podem surgir através de diferentes tipos celulares contribuindo ainda mais para heterogeneidade dessa população celular (Öhlund et al., 2017; Biffi & Tuveson, 2020; Sahai et al., 2020; Huang et al., 2022). Entre estas células estão as células estreladas pancreáticas, tipo celular de origem mesenquimal, comumente presente no pâncreas que se encontram quiescentes em homeostase (Jin et al., 2020). Elas são ativadas a partir de estresses ambientais causados por doenças inflamatórias como a pancreatite e na carcinogênese do ADP. Atualmente, já é bem descrito o processo que leva à diferenciação dessas células em myCAF; no entanto, essa população de myCAF originada das células estreladas parece possuir um perfil molecular diferente dos demais myCAF (Helms et al., 2022).

### 1.3.2 – O estroma do ADP: células e matriz extracelular (composição e organização)

A reação desmoplásica causada pela grande infiltração de fibroblastos presentes no microambiente combinado ao depósito excessivo de matriz extracelular é uma marca registrada

do ADP (Hosein et al., 2020). Geralmente, damos muita atenção para as interações celulares, mas a arquitetura tumoral também desempenha um papel central na progressão e resposta à terapia atuando como uma barreira física e molecular (Öhlund et al., 2013; Laklai et al., 2016; Almagro et al., 2022).

Os principais constituintes da matriz extracelular do ADP são colágeno (tipo I, II e IV) e fibronectina (Hosein et al., 2020). Altos níveis de colágeno fibrilar levam a pior sobrevida dos pacientes (Laklai et al., 2016; Whatcott et al., 2015). Até mesmo o diâmetro das fibras de colágeno pode impactar a resposta à terapia. Em um estudo realizado com modelos animais e pacientes, a maior espessura das fibras de colágeno próximas às células tumorais estava correlacionada a menor resposta à gemcitabina (Laklai et al., 2016). Outro grupo utilizou um inibidor de STAT3, proteína crucial para o depósito de matriz extracelular, combinado à gemcitabina resultando em melhora na sobrevida e diminuição do volume dos tumores dos animais (Nagathihalli et al., 2015). Foram realizadas inúmeras tentativas com terapias direcionadas para depleção ou remodelagem da matriz extracelular e, até o momento, não houve sucesso levando à descontinuidade apesar de resultados promissores em estudos *in vitro* e *in vivo* (Ramanathan et al., 2019; Van Cutsem et al., 2020).

Outra consequência deste estroma bastante fibrótico é o aumento da pressão intersticial afetando a perfusão e integridade do endotélio que por sua vez levam à hipóxia. Em um ambiente hipóxico, os altos níveis de HIF-1α e VEGF promovem um microambiente imunossupressor através da polarização de macrófagos para o fenótipo M2 e da inibição de linfócitos citotóxicos (Zandberg et al., 2021; Barsoum et al., 2014; Raggi et al., 2017; Ohm et al., 2003). Além disso, o endotélio disfuncional impede a chegada adequada dos quimioterápicos assim como impossibilita a extravasão dos linfócitos para dentro do microambiente tumoral.

### 1.3.3 – Componentes linfóide e mielóide no ADP

O ADP ainda é um dos poucos tumores refratários à imunoterapia e isso ocorre devido ao seu microambiente imunossupressor (Balachandran et al., 2019). Na maioria dos casos, a infiltração de linfócitos é baixa, especialmente de linfócitos CD8; além disso, a população de linfócitos Treg é bastante dominante (Karamitopoulou, 2019). Essa grande barreira física e molecular orquestrada pelos fibroblastos somada a um baixo *tumor mutation burden* (TMB) não explicam todo o problema (Lawlor et al., 2021). Os linfócitos CD8 entram em um estado

disfuncional heterogêneo que pode ou não ser definitivo (Schalck et al., 2022; Togashi et al., 2019; Kurachi, 2019; Wherry & Kurachi, 2015). Somado a isso, os linfócitos são fortemente modulados pelas interações com outras células imunes presentes no microambiente (Colligan et al., 2020).

As células mielóides representam a maior população imune no microambiente do ADP, sendo os macrófagos o principal tipo celular infiltrante. Esta característica contribui para a manutenção do microambiente imunossupressor, através da expressão tanto de moléculas inibidoras de checkpoint imunológico quanto promotoras da progressão tumoral (Kemp et al., 2020). Entretanto, os macrófagos também participam dos processos de apresentação de antígenos, secreção de citocinas e quimiocinas que atraem linfócitos citotóxicos desempenhando um papel anti-tumoral (Yang et al., 2021). Ainda considerando células fagocíticas e apresentadoras de antígeno, o microambiente do ADP é caracterizado pela escassez de células dendríticas; ademais, as poucas células dendríticas presentes são disfuncionais e incapazes de elicitar uma resposta efetiva dos linfócitos (Hedge et al., 2020). Translacionalmente, o acúmulo destas células disfuncionais favorece a formação de metástases (Kenkel et al., 2017). Recentemente, também foi identificado um fenótipo maduro de células dendríticas encontrado em estruturas terciárias linfóides, responsável pela ativação de linfócitos citotóxicos (Delvecchio et al., 2021). Contudo, ainda não está bem descrita a função dessa população pois ela também apresentou correlação positiva com células Treg, sugerindo um papel imunossupressor (Roth et al., 2020). Além disso, acredita-se que essa população possa ter origens diferentes dependendo do tipo de tumor, o que aumenta a complexidade da população (Cheng et al., 2021).

Além da composição celular, a distribuição espacial das células imunes no microambiente é de extrema importância para resposta anti-tumoral. A maior proximidade entre linfócitos CD8 e células tumorais está associada a melhor sobrevida dos pacientes (Hiraoka et al., 2014; Carstens et al., 2017). Contudo, esse cenário não é muito frequente no ADP onde os linfócitos CD8 tendem a ficar retidos no estroma (Ene-Obong et al., 2013; Hiraoka et al., 2014). Sendo assim, o melhor entendimento da distribuição das células imunes no microambiente pode permitir uma melhor estratificação dos pacientes e predição de prognóstico.

### 1.4 - As lesões precursoras do ADP e seus respectivos microambientes

O ADP surge a partir da progressão de neoplasias precursoras do epitélio ductal pancreático como as neoplasias intraepiteliais pancreáticas (PanINs), ou lesões císticas tais como as neoplasias mucinosas papilares intraductais (IPMNs) e as neoplasias císticas mucinosas (MCNs) (Hayashi et al., 2021; Connor & Gallinger, 2021). PanINs são encontradas próximas ao tumor e compartilham das mesmas alterações genéticas, especialmente *KRAS* mutada (Kanda et al., 2012). Apesar da alta frequência, essas lesões são muito pequenas, diferente das lesões císticas, dificultando diagnóstico pré-operatório. Outro fator que impede um *screening* adequado é justamente a capacidade dessas células precursoras colonizarem os ductos pancreáticos, inclusive regiões distantes ao tumor, semelhante ao processo de cancerização dos ductos que é bastante comum no ADP (Makohon-Moore et al., 2018).

O microambiente dessas lesões pré-malignas já apresenta semelhanças com os carcinomas, mas também possui aspectos intermediários únicos. Roth e colaboradores compararam a composição do infiltrado imunológico entre IPMN de baixo e alto grau, com IPMN associada ao carcinoma invasivo. Curiosamente, a presença de estruturas terciárias linfóides foi encontrada já nas lesões de baixo grau. Ao longo da progressão, houve alterações significativas na composição do infiltrado imunológico, seja peri-tumoral (restrito ao estroma) ou justatumoral (maior proximidade com as células tumorais), e na composição das estruturas terciárias linfóides. Os linfócitos Treg e as células dendríticas maduras apresentaram maior enriquecimento nas amostras de carcinoma. Além disso, a população de linfócitos citotóxicos diminuiu de forma gradual ao longo da progressão tumoral. Em contrapartida, os macrófagos demonstraram enriquecimento nas amostras de carcinoma, especialmente, nas regiões próximas às células tumorais (Roth et al., 2020).

Em um pré-print recente, Bell e colaboradores investigaram alterações celulares e moleculares nas PanINs utilizando transcriptômica espacial. Os fibroblastos foram o principal tipo celular infiltrando o microambiente e estavam em proximidade com os ductos neoplásicos. Além disso, os 3 subtipos de fibroblastos também foram identificados pela primeira vez em lesões pré-malignas de pacientes. Isso indica que os fibroblastos são os grandes responsáveis em iniciar a construção e modulação de um microambiente favorável à progressão tumoral (Bell et al., 2022).

## 2. JUSTIFICATIVA

O ADP é um tumor muito agressivo e letal, e poucos avanços relacionados a novos marcadores e melhora do prognóstico dos pacientes foram observados nas últimas décadas. Por outro lado, tem se tornado cada vez maior a quantidade e a qualidade de bancos contendo dados clínicos, histopatológicos e moleculares de pacientes oncológicos. Alguns destes bancos possuem, ainda, informações de lesões pré-malignas. Com isto, abriu-se a possibilidade de elucidar o complexo ecossistema formado ao longo da evolução tumoral. Neste contexto, investigar a composição e o status do microambiente tumoral em diferentes estágios da progressão do ADP pode fornecer informações básicas sobre a biologia destes tumores, bem como evidências clinicamente relevantes incluindo novos indicadores de prognóstico ou potenciais alvos terapêuticos.

## 3. QUESTÃO DE PESQUISA

Há diferenças na composição, interações celulares e organização do microambiente tumoral do ADP em diferentes estágios da doença?

## 4. HIPÓTESE

Nossa hipótese é de que existem variações significativas na composição, interações celulares e organização do microambiente tumoral em diferentes estágios da progressão do ADP, e que estas alterações estão associadas ao comportamento do tumor.

# 5. OBJETIVOS

## 5.1 – GERAL

Caracterizar o microambiente tumoral do ADP em diferentes etapas da carcinogênese.

## 5.2 - ESPECÍFICOS

A partir de *datasets* de amostras de tecido normal, tecido adjacente ao tumor, ADPs primários e lesões metastáticas:

**a)** Identificar os diferentes tipos celulares que compõem o microambiente e seus respectivos estados celulares

**b)** Construir trajetórias celulares para investigar o processo de diferenciação entre os diferentes estados celulares

**c)** Predizer as interações celulares existentes no microambiente tumoral do ADP

## 6. ARTIGO CIENTÍFICO

(manuscrito será submetido ao repositório de preprint bioRxiv; as figuras principais com suas respectivas legendas foram inseridas ao longo do artigo para facilitar a leitura e entendimento do mesmo; as figuras suplementares se encontram ao final do manuscrito)

# Integrated single-cell analysis highlights cell composition dynamics and complex intercellular communication in pancreatic cancer progression

Gabriel F. Pozo de Mattos Pereira[1,2], Eduardo Cremonese Filippi-Chiela[1,2,3,4], Alessandro Bersch Osvaldt[5,6,7], Simone Marcia dos Santos Machado[8]

[1]Graduate Program in Physiology, Universidade Federal do Rio Grande do Sul. Ramiro Barcelos, 2600. 90035-003 Porto Alegre / RS-Brazil

[2]Experimental Research Service, Hospital de Clínicas de Porto Alegre. Ramiro Barcelos 2350. 90035-903 Porto Alegre / RS-Brazil.

[3]Department of Morphological Sciences, Universidade Federal do Rio Grande do Sul. Sarmento Leite 500. 90035-903 Porto Alegre / RS-Brazil.

[4]Biotechnology Center, Universidade Federal do Rio Grande do Sul, Porto Alegre, RS, Brazil.

[5]Medical School, Universidade Federal do Rio Grande do Sul, Porto Alegre, RS, Brazil.

[6]Digestive Surgery Service, Biliary and Pancreas Group, Hospital de Clínicas de Porto Alegre, Porto Alegre, RS, Brazil.

[7]Graduate Program in Medicine: Surgical Sciences, Universidade Federal do Rio Grande do Sul, Porto Alegre, RS, Brazil.

[8]Pathology Service, Hospital de Clínicas de Porto Alegre, Porto Alegre, RS, Brazil.

**Abstract**

Pancreatic ductal adenocarcinoma (PDAC) is a deadly disease well known for its heterogeneous tumor microenvironment (TME). Single-cell RNA sequencing (scRNA-seq) has been extensevily used to characterize the intratumor and intertumor heterogeneity of PDAC. However, TME cellular composition dynamics and intercellular communication during PDAC's progression are not fully comprehended. Here, we integrated scRNA-seq data from four different datasets containing four distinct tissue sites. We observed a higher proportion of memory CD8 T cells in adjacent tissue samples than malignant samples. On the other hand, regulatory T cells and dysfunctional CD8 T cells ($GZMK^+$ CD8) were among the most prevalent cell type in malignant samples. Macrophages were the most abundant cell type in the myeloid component. We identified four clusters of macrophages; pseudotime analysis suggested a potential common origin for $C1Q^+$ Macro and $SPP1^+$ Macro. As expected, CAFs (cancer-associated fibroblasts) were enriched in PDAC. Trajectory analysis for stromal cells revealed a transition from stellate cells to myofibroblastic CAFs (myCAF). After refined cell type annotation, we built cell-cell interactions network that unraveled CAFs as the major source of extracellular signals. In contrast, CD8 T cells were the most frequent final destination for multiple signals in the TME. Our results provide a refined characterization of cell composition and cell-cell interaction dynamics for PDAC microenvironment.

**Keywords:** single-cell sequencing, pancreatic ductal adenocarcinoma, tumor microenvironment, intercellular communication, cell composition

## 1. Introduction

Pancreatic ductal adenocarcinoma (PDAC) represents 90% of pancreatic neoplasms (**Kleeff *et al.*, 2016**). Most patients already present metastatic lesions at the moment of diagnosis and around 35% have locally advanced disease (**Park *et al.*, 2021**). Late diagnosis prevents patients from undergoing resection, which is available only for 15% of the cases. The absence of specific biomarkers and symptoms impedes effective screening for early diagnosis. The 5-year survival rate just reached 10% last year despite all efforts (**Siegel *et al.*, 2021**). These challenges arise from the highly heterogeneous tumor microenvironment (TME) observed in PDAC (**Ho *et al.*, 2020**).

TME is a complex ecosystem formed by stromal cells, immune cells, and tumor cells beyond the extracellular matrix (ECM). Non-tumoral cells engage in heterotypic intercellular interactions among themselves and with malignant cells. TME composition is dynamic throughout carcinogenesis, from premalignant lesions to established metastasis (**Roth *et al.*, 2020; Schlesinger *et al.*, 2020; Lin *et al.*, 2020, Lee *et al.*, 2021)**. Furthermore, it can provide valuable information about tumor progression, response to therapy, and even prognosis (**Grünwald *et al.*, 2021; Raghavan *et al.*, 2021; Wang *et al.*, 2021; Wu *et al.*, 2021; Bagaev *et al.*, 2021; Luca *et al.*, 2021; Storrs *et al.*, 2022**). PDAC TME is characterized by the high prevalence of cancer-associated fibroblasts (CAFs) and myeloid cells, which sustain malignant cells and promote an immunosuppressive TME associated with few cytotoxic lymphocytes (**Ho *et al.*, 2020**). However, the TME of metastatic lesions is less explored. A few studies found distinct TME composition suggesting that these lesions can be as much heterogeneous as primary tumors (**Lin *et al.*, 2020, Lee *et al.*, 2021; Raghavan *et al.*, 2021**).

In order to get an in-depth characterization of the dynamic microenvironment, we integrated multiple publicly available datasets of scRNA-seq across different biological conditions containing samples from normal pancreatic tissue, adjacent tissue, PDAC, and metastatic PDAC. Our data integration revealed distinct global composition and within components (*e.g.*, lymphoid cells, myeloid cells) between biological conditions. The microenvironment composition of adjacent tissue samples drastically differed from normal tissue as a host response against nearby tumor growth. PDAC samples showed a high interpatient heterogeneity unraveling two groups: immune-rich and immune-depleted. Pseudotime analysis of monocytes and macrophages revealed a transition from monocytes to macrophages that further differentiate into $SPP1^+$ or $C1Q^+$ macrophages. Moreover, cell trajectory also identified that cancer-associated myofibroblasts (myCAFs) are potentially derived from pancreatic stellate cells. Finally, cell-cell interaction analysis pointed out the CAFs as one of the main sources of extracellular signaling within the tumor microenvironment in PDAC. Furthermore, we identified ligand-receptor (L-R) pairs that may explain the differences in cell composition between distinct biological conditions.

## 2. Material and Methods

### 2.1 - Data download

We downloaded 4 publicly available scRNA-seq data from previous studies: GSE155698 (**Steele *et al.*, 2020**), GSE154778 (**Lin *et al.*, 2020**), GSE156405 (**Lee *et al.*, 2021**), and PRJA001063 (**Peng *et al.*, 2019**). Pre-processed data were obtained for GSE155698, GSE154778, and GSE156405 from GEO, while normalized counts for PRJA001063 were obtained from the TISCH database (**Sun *et al.*, 2021**). Single-cell analysis was performed with *Seurat* (**Stuart *et al.*, 2019**).

### 2.2 - Data processing, normalization, integration, and clustering

As we had access to normalized data for PRJA001063, filtering and processing weren't necessary. For the rest, each dataset was processed separately before integration. We established a cutoff to retain only high-quality cells in our data: cells with less than 1000 and more than 60.000 counts, less than 500 and more than 8000 features, and cells with more than 50% of mitochondrial genes were filtered out. Normalization was performed with a scale factor of 10.000 and after this step, we merged the datasets. Our merged *Seurat object* contained ~140k cells. Next, we identified the 3000 *HVG* (highly variable genes) which will be used downstream for dimensionality reduction. Before, scaling the data we assessed the cell cycle score and regressed out cell cycle difference as recommended in the tutorial. Integration and batch effect correction were conducted with *Harmony* (**Korsunsky *et al.*, 2019**) as follows: *RunHarmony* (*vars.to.regress = "sample_ID"*). The optimal number of PCA (principal components) was defined with the *Elbowplot* function. Initially, cells were clustered using the Louvain algorithm and top 50 PCA dimensions via "FindNeighbors" and "FindClusters" with a resolution of 0.3. Clusters were manually annotated based on canonical marker genes. Differentially expressed genes (DEGs) were identified via "FindAllMarkers" (parameters - *min.pct = 0.25, logFCthreshold = 0.5, test.use = "MAST"*) function.

### 2.3 - Copy-number variation score (CNV score)

Infercnvpy (https://github.com/icbi-lab/infercnvpy) is a plugin derived from *inferCNV* library to infer copy number variation from single-cell transcriptomics data. We downloaded the GTF file from the Xena browser to obtain the chromosome location for each gene in our matrix. Then, we followed the *infercnvpy* tutorial and defined lymphoid cells as our reference. Ductal cells with a 'cnv_score' higher than 0.009 were classified as malignant cells.

### 2.4 - Gene signatures with UCell

Gene signature scores were assessed with *UCell* (**Andreatta M & Carmona SJ, 2021**), an R package, via *AddModuleScore_UCell* function that calculates the score of the geneset for each cell individually.

### 2.5 - Functional enrichment analysis

We filtered the top 100 differentially expressed genes and performed annotation with *clusterProfiler* (**Yu *et al.*, 2012**) package. Our parameters were, *ontology* = 'Biological Processes' and *pvalueCutoff* = '0.05'.

### 2.6 - Trajectory analysis with Monocle

Cell trajectories for myeloid (monocytes and macrophages) and stromal cells (stellate cells and fibroblasts) were constructed with *monocle2* (**Van Der Berge *et al.*, 2020**). Our integrated gene matrix was exported from *Seurat* and used as input to construct the CellDataSet object. For cell ordering, we applied the differentialGeneTest (*cutoff* of q<0.001) function to determine the variable genes. Dimensionality reduction was performed without normalization, as it was previously done with *Seurat*, and the DDRTree reduction method.

### 2.7 - Cell-cell interactions with CellChat

We used our scRNA-seq data to predict potential cell-cell interactions with the *CellChat* (**Jin *et al.*, 2021**) R package. For input, we provided our scRNA-seq matrix with all 38 cell types previously annotated. First, we constructed separate cellchat objects for each condition (AdjTumor, PDAC, and MET) as recommended in the tutorial. Afterward, we conducted a comparative analysis to infer differentially enriched ligand-receptor interactions within the TME. We visualized the outgoing signaling and incoming signaling strength of the cell types between the different conditions via the *netAnalysis_signalingRole_scatter* function. Furthermore, we identified the significantly enriched pathways L-R interactions across all conditions using the *netAnalysis_signalingRole_heatmap* function, setting the options *pattern* = "*all*" to aggregate the incoming and outcoming signaling strengths.

## 3. Results

### 3.1 - scRNA-seq integration reveals a heterogeneous microenvironment between conditions and within PDAC patients

We integrated 4 public scRNA-seq datasets, reaching 11 samples of normal pancreatic tissue (Normal), 3 adjacent tissue (AdjTumor), 56 primary tumors (PDAC), and 8 metastatic lesions (MET) and performed different types of single-cell analysis including clusterization, cell composition, cell trajectory inference and cell-cell interaction prediction in a total of 137,699 cells from 78 patients (**Figure 1A-E; Figure 2A**). We found 11 metaclusters: acinar cells (n=3,803), ductal cells (n=50,211), endocrine cells (n=775), endothelial cells (n=9,942), stellate cells (n=7,417), fibroblasts (n=10,289), myeloid cells (n=22,205), T/NK cells (n=24,124), B cells (n=4,767), plasmablasts (n=2,090) and mast cells (n=2,076) (**Figure 2A**).

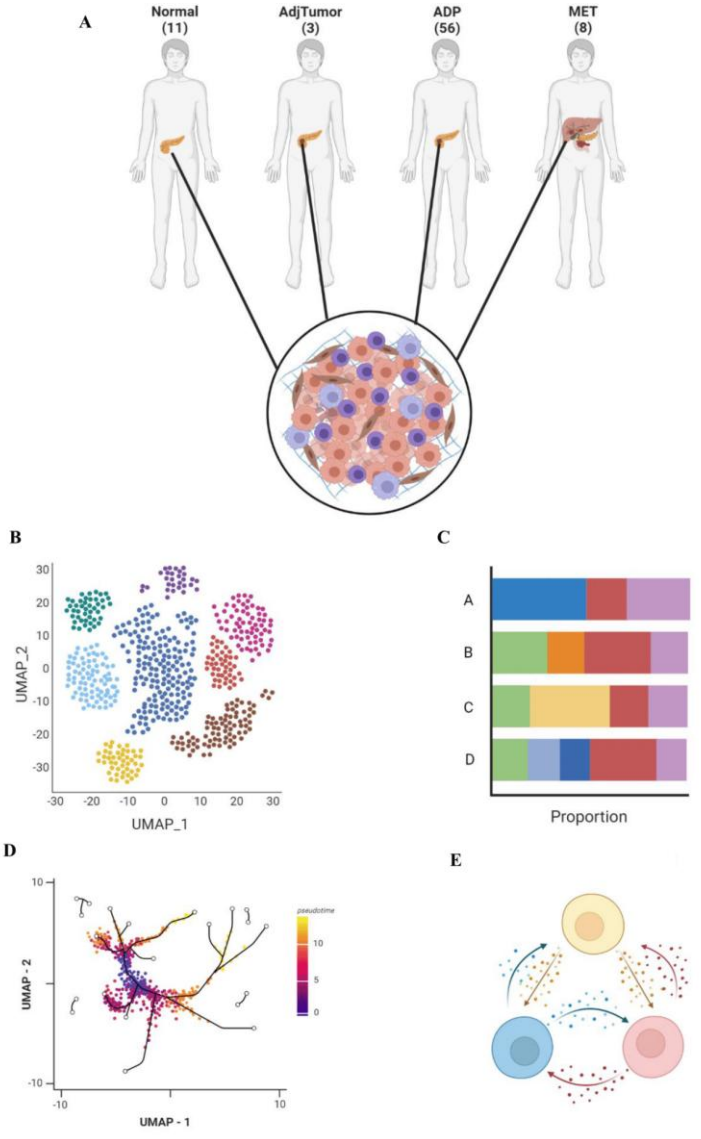



**Figure 1 - Workflow of the study. A**) Integrated cohort. **B**) Clusterization. **C**) Cell composition. **D**) Cell trajectory. **E**) Cell-cell interactions.

Although there was a big difference in the number of cells derived from each condition (**Supplementary Figure 1A-B**), we removed the potential batch effects with *harmony*, so every metacluster is composed of all 4 biological conditions and datasets. The cellular composition was remarkably distinct between normal tissue and adjacent tissue, the former enriched by ductal cells and the latter marked by high infiltration of T/NK cells. Furthermore, TME composition between primary tumors and adjacent tissue was quite similar except for the enrichment of ductal cells and fibroblasts which is a hallmark of PDAC (**Figure 2B**). Even though the stacked bar chart revealed similar features between PDAC and MET, the latter exhibited a poor microenvironment dominated by ductal cells, while PDAC samples showed a diverse composition enriched by stromal and immune cells (**Figure 2B**). Within PDAC, there were two main types of TME compositions: one marked by high infiltration of T/NK cells and low infiltration of fibroblasts/stellate cells, and the other marked by poor infiltration of T/NK cells and enriched in fibroblasts/stellate cells (**Figure 2C**).

The metaclusters were classified by the expression of known canonical markers (**Figure 2D**). Moreover, gene set enrichment analysis was applied to elucidate the role played by each metacluster in the TME. As expected, ductal cells were associated with cell cycle activation pathways, p53, DNA repair, gluconeogenesis, and MYC targets. Myeloid cells were linked to inflammatory pathways (***e.g*** TNFα/NFK**β**, JAK/STAT), while fibroblasts were linked to epithelial-mesenchymal transition (EMT), hypoxia, and angiogenesis (**Supplementary Figure 1C**). In this first round of clusterization, some cell types remained together, like neutrophils, monocytes, macrophages, and dendritic cells, which belong to the myeloid metacluster, and the lymphoid metacluster (**Figure 2E**).

In summary, we found major differences in the microenvironment cell composition between distinct biological conditions and also identified high transcriptional heterogeneity within the metaclusters reflected by diverse pathway enrichment scores. To refine the characterization of each metacluster, we subsetted and reclustered all metaclusters except B cells, plasmablasts, mast cells, and endocrine cells because we already captured their heterogeneity. As the ductal metacluster contained both malignant and non-malignant cells, we used *inferCNVpy* to distinguish these populations. Ductal cells with a *cnv_score* higher than 0.009 and high expression of *KRT19*, *FXYD3*, and *CEACAM6* were defined as malignant ductal cells. Normal ductal cells retained expression of *CFTR*, *FXYD2*, and *AMBP* (**Supplementary Figure 2A**).

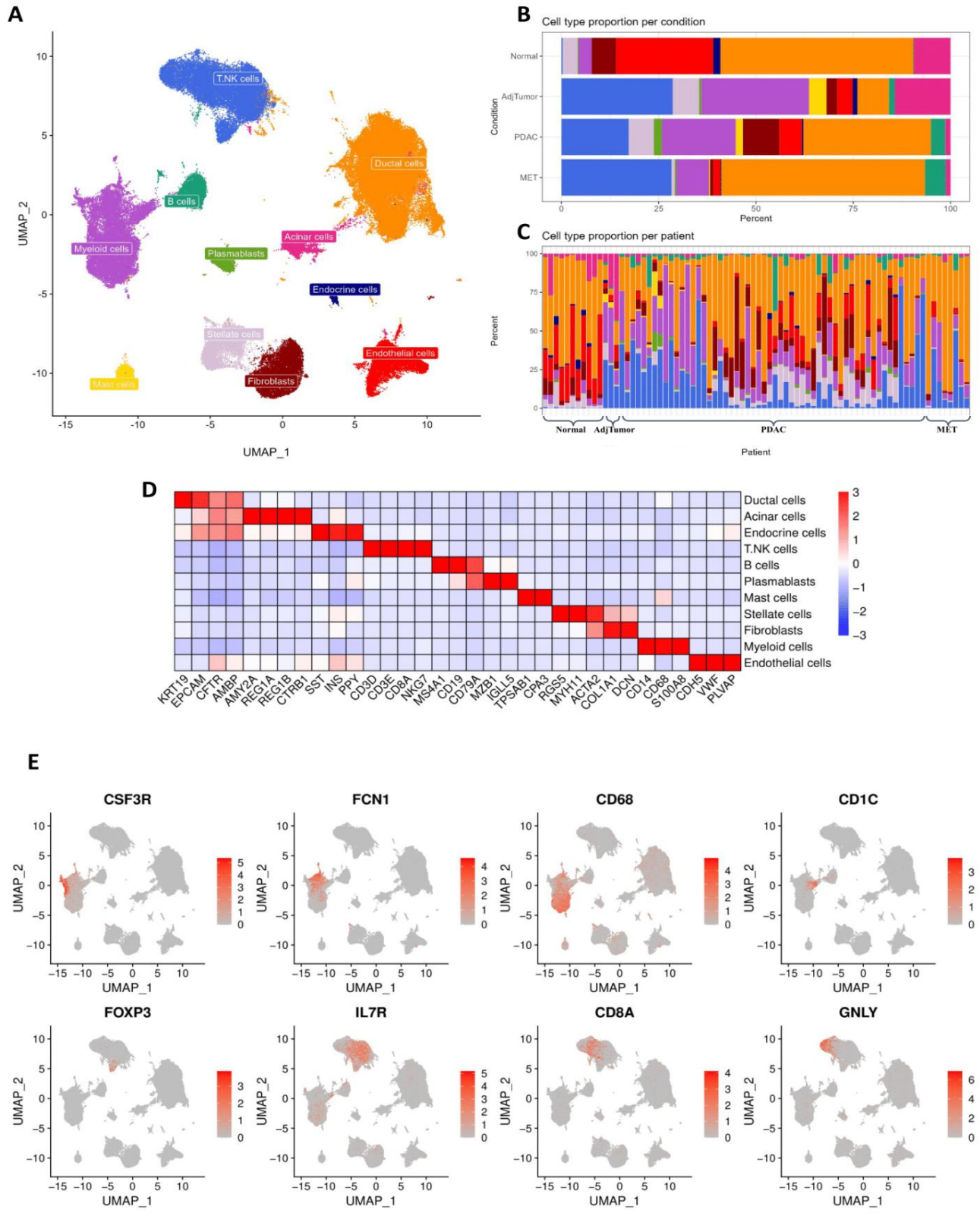



**Figure 2** – **Metaclusters determination and characterization**. **A**) UMAP, Uniform Manifold Approximation, and Projection, of 137,699 cells derived from data integration across 78 samples. **B**) Cell type quantification across the four different conditions: Normal n=11; AdjTumor n=3; PDAC n=56; MET n=8. **C**) Cell type quantification across 78 individuals. **D**) Mean normalized expression of canonical markers for each cell type. **E**) Feature plot with log-normalized expression of gene markers respective to different myeloid (*CSF3R*, *FCN1*, *CD68*, *CD1C*) and lymphoid (*IL7R*, *CD8A*, *FOXP3*, *GNLY*) lineage cells.

### 3.2 - Effective anti-tumor immunity and anti-tumor memory are stronger in adjacent tissue than in malignant tissue

To better understand the complete landscape of lymphoid cells, we subsetted the T/NK metacluster. Thirteen clusters were recovered in total. Five distinct clusters of CD8 T cells, four distinct clusters of NK cells, one big cluster of CD4 T cells, one cluster of CD4 Treg cells, one cluster of IFN T cells, and one cluster of mucosal-associated invariant T cells (MAIT) cells (**Figure 3A**).

CD4 Treg cells were enriched in malignancy (**Figure 3B-C**). These cells showed high expression of well-known immunosuppressive markers, which include *CTLA4*, *TIGIT*, *FOXP3*, and *TNFRSF18.* (**Figure 3D**). In addition, a big cluster of CD4 T cells overexpressed genes associated with a naive state, *CCR7*, *LTB*, *TCF7*, and *SELL*, therefore labeled as Naive-like CD4 (**Figure 3D**). This cluster was the most dominant in PDAC and MET cases (**Figure 3B**). We also detected a small cluster of early activated T cells identified by high interferon-produced protein levels (**Figure 3A and 3D**). MAIT cells are innate-like T cells recognized by *TRBV7-6*, *TRBV7-2*, and *TRBV7-9* genes, which are involved with antigen recognition (**Figure 3D**). These cells were exclusive to Lee's dataset (**Lee *et al.,* 2021**). This reinforces our robust data integration as we were able to find similarities between the datasets, but also retain biological heterogeneity (**Supplementary figure 3A-B**).

CD8 T cells could be divided regarding their functional states. $GZMK^+$ CD8 cluster expressed *GZMK*, *EOMES*, and *TIGIT*, and has been linked to the exhausted phenotype in PDAC and aging (**Steele *et al.,* 2020; Mogilenko *et al.,* 2021**). Moreover, it was the most common subtype of CD8 T cells in malignancy (**Figure 3B-D**). The effector CD8 cluster was characterized by low expression of *GZMK* and high expression of cytotoxic markers like *NKG7* and *GZMH* **(Figure 3D)**. Strikingly, the most significant difference in the TME composition between the adjacent tissue and the malignant ones was the proportion of memory CD8 T cells, which was more prevalent in the first condition (**Figure 3B**). This population was identified by the high levels of *CXCR6*, *ITGA1*, and *CD69* **(Figure 3D)**. A pan-cancer analysis also observed the enrichment of memory CD8 T cells in adjacent tissue compared to tumor tissue (**Aran *et al.,* 2017**). $KLRB1^+$ CD8 cluster was identified by *KLRB1* overexpression and exhibited a similar profile to the $GZMK^+$ CD8 cluster. A recent scRNA-seq analysis of glioblastoma unraveled *KLRB1* as a potential driver of immunosuppression (**Mathewson *et al.,* 2021**). One particular population (labeled as Naive-like CD8) was difficult to classify since it showed a high transcriptomic heterogeneity (coexpression of memory and naive markers, but low levels of T cell activation markers) and clustered close to the naive-like CD4 T cells (**Figure 3A**).

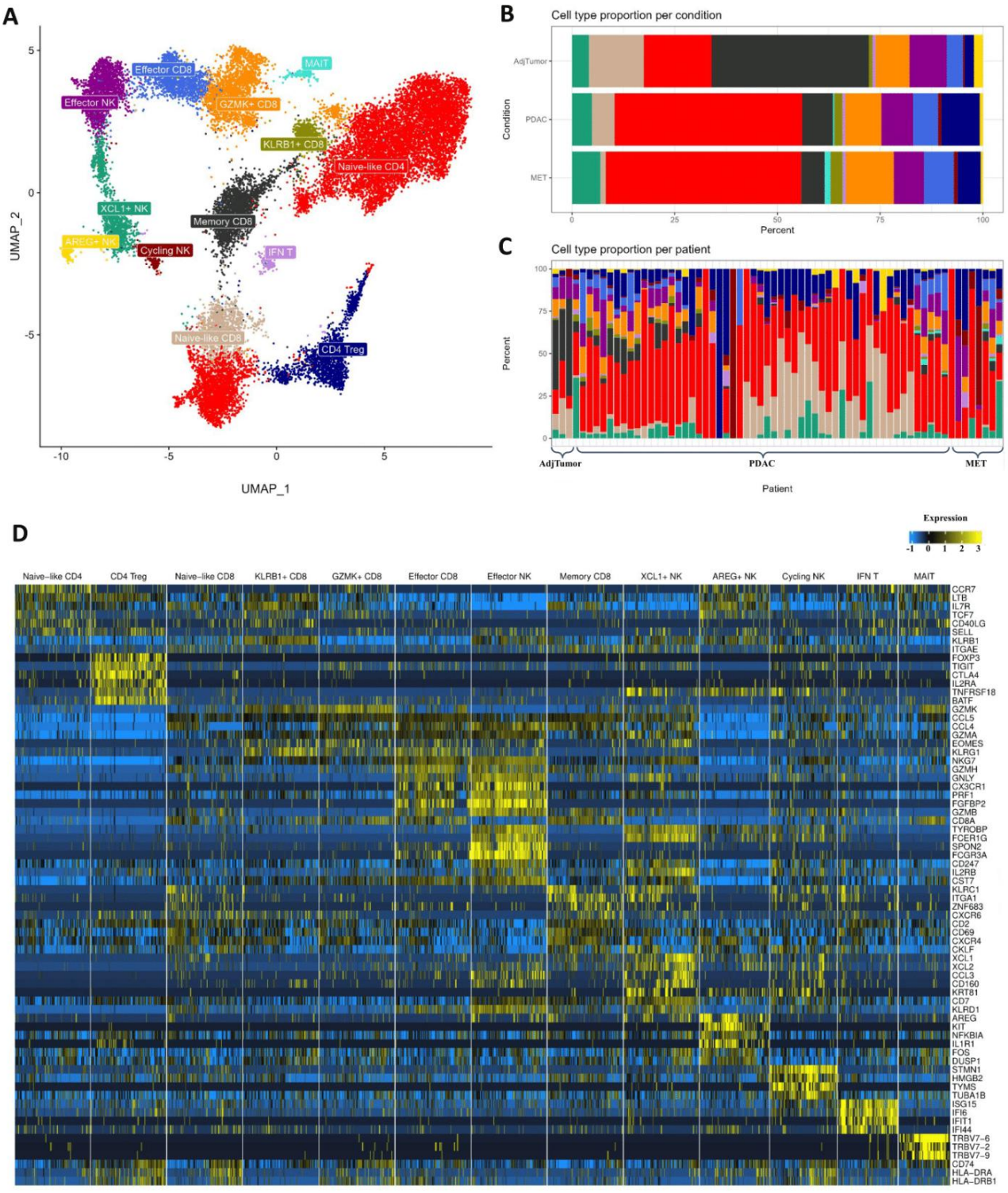



**Figure 3 – Characterization of lymphoid cells in PDAC-associated lesions. A**) Reclusterization of lymphoid cells (n = 24.124). **B**) Cell type quantification across the four different conditions. **C**) Cell type quantification across individuals. **D)** Single-cell resolution heatmap for the markers for each cluster.

Unlike the effector CD8 T cells, the effector NK cells retained high levels of activation and cytotoxicity genes (*GZMA*, *GZMB*, *CX3CR1*, *PRF1*, and *GNLY*) **(Figure 3D)**. Interestingly, a small subset of NK cells - labeled as AREG$^{+}$ NK - characterized by high expression of *AREG*, *KIT*, and *NFKBIA*, showed high levels of multiple T cell markers (*CCR7*, *IL7R*, *LTB*) (**Figure 3D**). To avoid misinterpretation, we searched for the expression of *CD3D*, *CD4*, and *CD8A* in this cluster, but no expression was found. Besides, this cluster retained the expression of *FCER1G* which is a marker for NK cells (**Supplementary Figure 3C**). XCL1$^{+}$ NK cluster had increased levels of *XCL1* and *XCL2* which are chemokines that coordinate the infiltration of dendritic cells into the TME (**Lei & Takahama, 2012; Böttcher *et al.*, 2018**). Finally, we detected a few actively cycling NK cells (*MKI67*, *TOP2A*, and *STMN1*) (**Figure 3A-D**).

To comprehensively understand the role of each one of these clusters, we built four distinct gene signatures associated with well-known states of lymphoid cells: naive-like, memory, effector, and exhaustion (**Supplementary figure 3D-E**). Naive-like and memory signatures have matched almost perfectly with their respective clusters (**Figure 4A**). As we previously discussed, NK cells remained activated while CD8 T cells couldn't keep it up **(Figure 4A, effector signature)**. Next, we compared the signature scores between conditions. We detected that effector anti-tumor immunity was more robust in the adjacent tissue than the malignant tissue, and the same result was observed for anti-tumor memory. In contrast, both naive-like and exhaustion scores were higher in metastatic samples (**Figure 4B**). Overall, our data reveal that PDAC and MET are dominated by dysfunctional CD8$^{+}$ T cells (GZMK$^{+}$ CD8), CD4 Tregs, and naive-like CD4$^{+}$ T cells forming a highly immunosuppressive TME, while adjacent tissue is composed mainly of memory CD8$^{+}$ T cells.

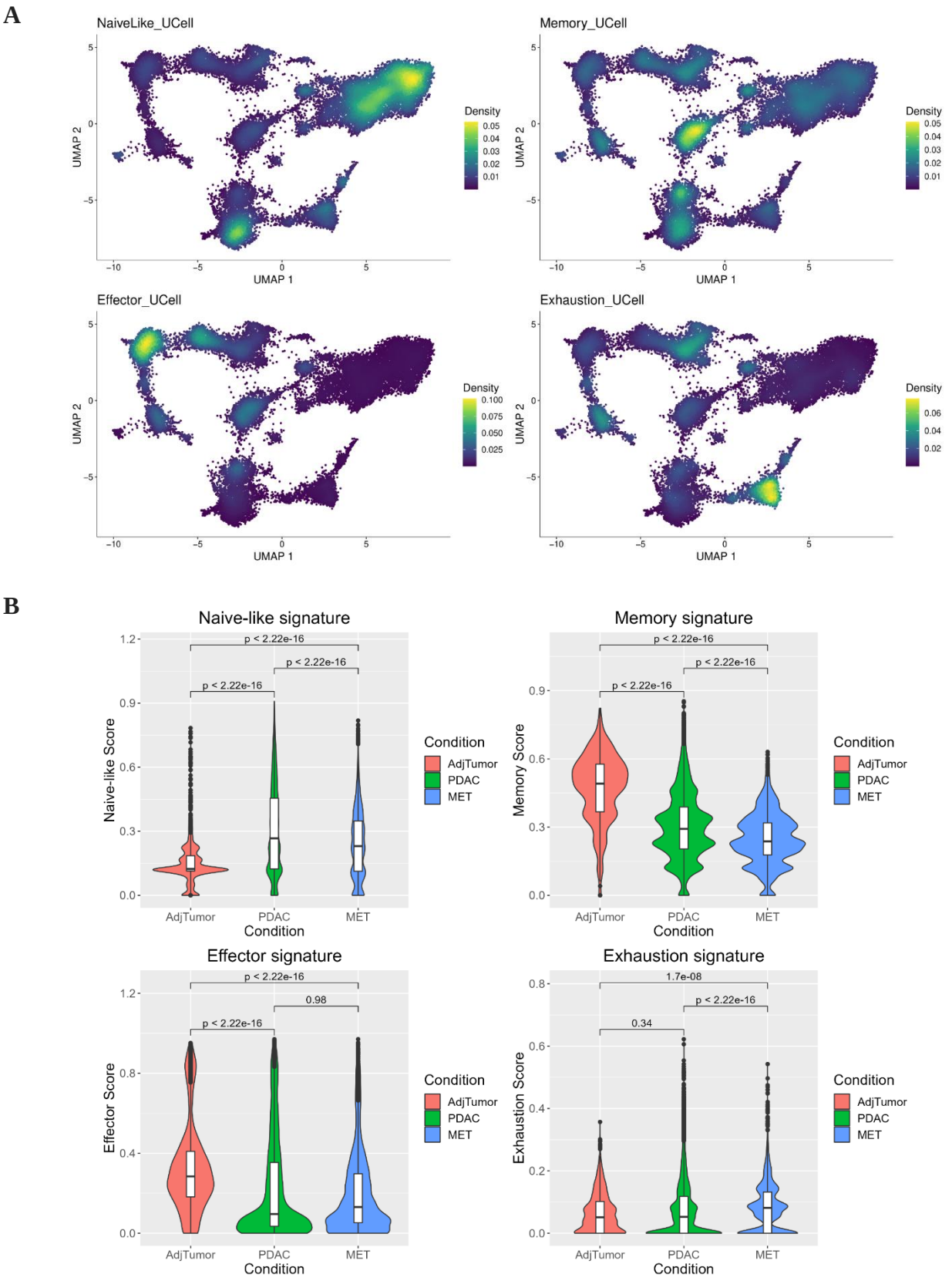



**Figure 4 – Immune signatures for lymphoid cells in PDAC-associated lesions. A)** Density plot for Naive-like, Memory, Effector, and Exhaustion signatures. Signature scores were calculated by each cell. **B)** Comparison of each signature score between AdjTumor, PDAC, and MET. Kruskal-Wallis test was performed for statistical analysis.

### 3.3 - Myeloid component is enriched by APOE$^+$ tumor-associated macrophages and conventional dendritic cells type II

Myeloid cells play a pivotal role in PDAC progression, sustaining an immunosuppressed microenvironment (**Kemp *et al.*, 2021**). Collectively, we identified 11 distinct clusters corresponding to four different cell types: macrophages, dendritic cells, monocytes, and neutrophils, differentially distributed between conditions (**Figure 5A-C**). Macrophages were clustered into C1Q$^+$, SPP1$^+$, APOE$^+$, IL1B$^+$, and IFN Macro. We also found two subpopulations of monocytes, classical and non-classical, distinguished by the expression of *CD14* and *FCGR3A* (CD16), respectively. Lastly, neutrophils were identified based on *CSF3R* and *FCGR3B* expression (**Figure 5D**).

Comparing the cellular composition among the different conditions, we observed a progressive increase in the SPP1$^+$, IL1B$^+$, and APOE$^+$ populations together with a decrease in the C1Q$^+$ population from normal tissue to metastasis. Additionally, IL1B$^+$ macrophages and CD14$^+$ monocytes showed enrichment in the metastatic tissue (**Figure 5B-C**). Next, we performed functional enrichment analysis to uncover the role of these populations. SPP1$^+$ macrophages were related to response to hypoxia, glycolytic process, and purine metabolism. C1Q$^+$ cells expressed genes associated with antigen presentation, MHC-II, and complement system (**Supplementary table**). A pan-cancer single-cell analysis identified a correlation between angiogenesis-related genes and SPP1$^+$ macrophages; furthermore, this population also showed worse survival for several cancer types (**Cheng *et al.*, 2021**). On the other hand, C1Q$^+$ macrophages exhibited a higher score for phagocytosis-related genes (**Cheng *et al.*, 2021**). Both CD14$^+$ monocytes and IL1B$^+$ were strongly associated with inflammatory pathways (**Supplementary table**).

It is well-established that monocytes can infiltrate the TME and differentiate into macrophages (**Yang & Zhang, 2017; Robinson *et al.*, 2021**). To better understand macrophage subpopulations and the sources of macrophage heterogeneity, we constructed a cell trajectory with the *monocle* package. As expected, pseudotime analysis revealed a transition from CD14$^+$ monocytes into IL1B$^+$ macrophages (**Figure 5E; and Supplementary figure 4A**). It was evidenced by the increased expression of *CD68* and *GPNMB*, and decreased expression of *S100A8* and *S100A9* (**Supplementary figure 4B**), followed by a branch that segregates C1Q$^+$ macrophages from SPP1$^+$ macrophages. Strikingly, the APOE$^+$ subpopulation contributed to both distinct cell fates (SPP1$^+$ and C1Q$^+$), suggesting a potential common origin between these clusters. In other tumors, *APOE* expression is restricted to C1Q$^+$ macrophages (**Revel *et al.*, 2022**), but it doesn't seem to be the case for PDAC as we detected coexpression of both SPP1$^+$ and C1Q$^+$ related genes within APOE$^+$ macrophages (**Supplementary figure 5C**). Besides, *APOE* overexpression is a hallmark of tumor-associated macrophages across multiple neoplasms (**Cheng *et al.*, 2021; Nalio Ramos *et al.*, 2022**),

including PDAC (**Steele *et al.*, 2020; Kemp *et al.*, 2021**). We identified an intermediate state of $CD14^+$ monocytes characterized by high expression of *CD163* and MHC-II genes (*HLA-DRA*, *HLA-DPB1*, *HLA-DPA1*) (**Figure 5E; and Supplementary figure 4C**). Finally, we searched for the genes that determined the two distinct cell fates observed in branch 1. The enrichment for markers of the complement system (*C1QA*, *C1QB*, *C1QC*), MHC-II (*CD74*, *HLA-DRA*, and *HLA-DPA1*), *FOLR2*, *SEPP1* led to differentiation of $C1Q^+$ macrophages, while enrichment for immunosuppressive (*S100A8*, *S100A9*, *VCAN*, *MARCO*), EMT (*FN1*, *TIMP1*, *VIM*) and response to stress markers (*SPP1*, *PLIN2*, *NUPR1*) led to differentiation of $SPP1^+$ macrophages (**Figure 5F; and Supplementary figure 4D**).

One of the main difficulties in eliciting effective anti-tumor immunity in PDAC is caused by the sparsity of dendritic cells (DC) (**Hedge *et al.*, 2020**). We identified three subpopulations of dendritic cells: (i) cDC2 (conventional dendritic cells type II), which is the most common phenotype of DC found in PDAC, characterized by high levels of *CD1C*, *FCER1A*, *CLEC10A*, and MHC-II markers (*CD74*, *HLA-DRA*); (ii) $LAMP3^+$ DC, which overexpress genes involved in DC maturation, like *LAMP3*, *IL7R*, *BIRC3*; and (iii) cDC1 (conventional dendritic cells type I), which express *XCR1*, *CLEC9A*, *IRF8*, *BATF3*, and *CPVL*, suggesting a role in antigen cross-presentation (**Figure 5A-D**). *BATF3* is required for effector T cell trafficking and response against malignancy (**Spranger *et al.*, 2017**). Moreover, *XCR1* is expressed in response to NK-secreted *XCL1* and *XCL2*, leading to DC migration into the tumor. $LAMP3^+$ DC also showed high levels of chemokines that recruit lymphocytes into tumors (*CCL17*, *CCL19*, *CCL22*) and immunosuppressive markers (*IDO1*, *CD274*), indicating a potential regulatory role in inhibiting cytotoxicity (**Supplementary figure 5A**).

Finally, we constructed a cell trajectory to comprehend the development of DC clusters. Surprisingly, cDC2 showed a progressive transition towards both cDC1 and $LAMP3^+$ DC, evidenced by decreased expression of *CD1C* and *FCER1A*, and increased expression of *LAMP3*, *CCR7* ($LAMP3^+$ cells), *XCR1*, and *CLEC9A* (cDC1 cells) (**Figure 5G-H; and Supplementary figure 4B**). This result comes in agreement with a recent pan-cancer analysis that identified cDC2 as the potential origin for $LAMP3^+$ DC (**Cheng *et al.*, 2021**). The transition from cDC2 to cDC1 was marked by late overexpression of typical cDC1 markers (*IRF8*, *BATF3*, *DNASE1L3*) (**Figure 5H; and Supplementary figure 5D**). Curiously, a few cDC2 cells expressed the above mentioned genes related to the cDC1 differentiation state (**Supplementary figure 5C**). This potential transition could be explained by the different ontogeny of cDC2 cells present in the TME (**Bosteels *et al.*, 2020**).

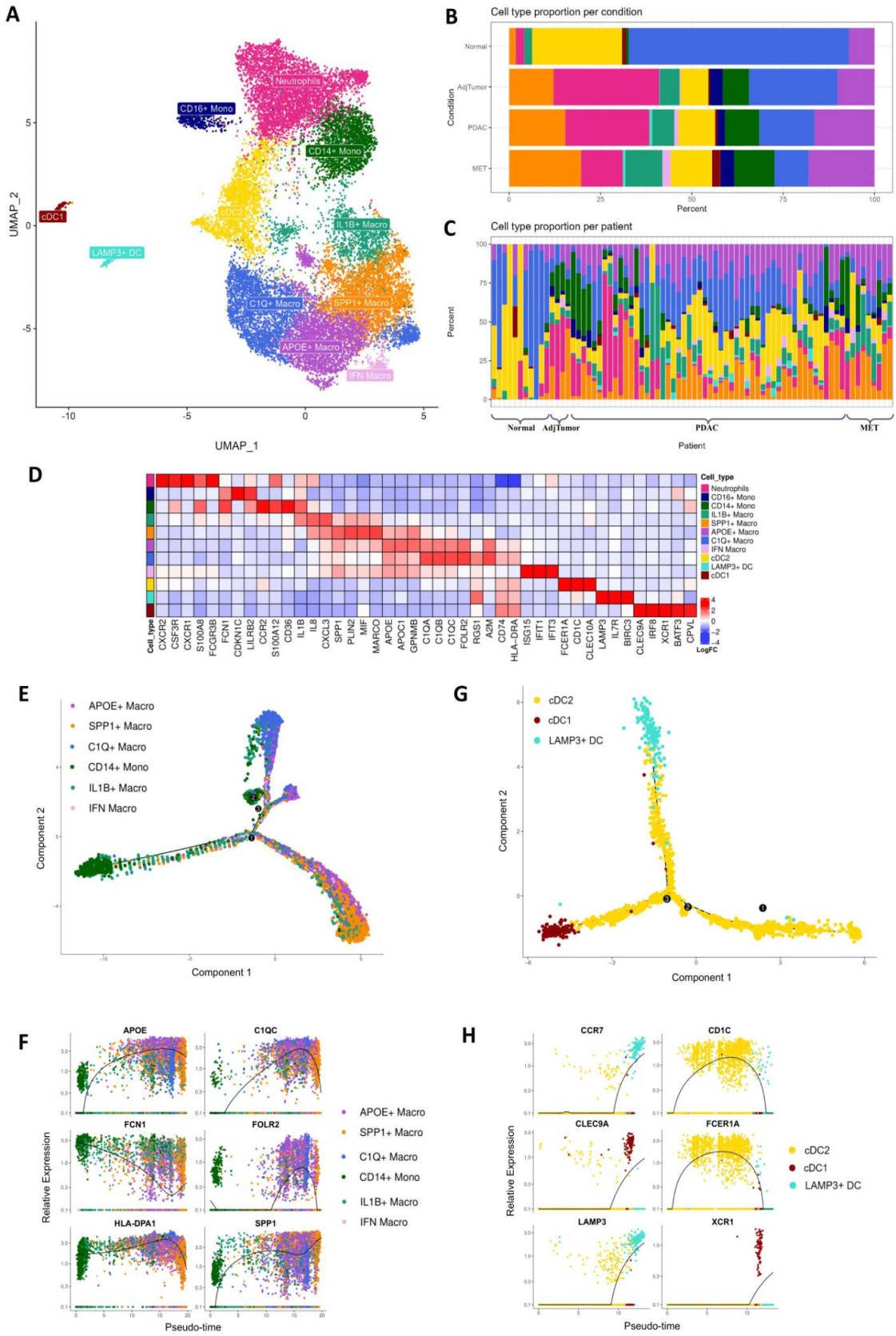



**Figure 5 - Characterization of myeloid cells in PDAC-associated lesions. A)** Reclustered myeloid cells **B**) Cell type quantification across the four different conditions. **C**) Cell type quantification across individuals. **D**) Mean normalized expression of markers for each cluster. **E**) Cell trajectory analysis for monocytes and macrophages. **F**) Expression of genes that change as a function of pseudotime for

monocytes and macrophages. **G**) Cell trajectory analysis for dendritic cells. **H**) Expression of genes that change as a function of pseudotime for dendritic cells.

### 3.4 - myCAFs are enriched in PDAC and can be derived from pancreatic stellate cells

PDAC is characterized by high desmoplasia due to the enrichment of CAFs and pancreatic stellate cells (**Zhan *et al.*, 2017**; **Thomas & Radhakrishnan, 2019; Zhang *et al.*, 2019**). We identified eight clusters of stromal cells in total. Three subpopulations of endothelial cells (ACKR1$^+$ Endo, CXCL12$^+$ Endo, and FABP5$^+$ Endo), three subpopulations of fibroblasts (myCAF, iCAF, and Cycling myCAF), and two subpopulations of pancreatic stellate cells (RGS5$^+$ Stellate and MYH11$^+$ Stellate) (**Figure 6A**).

ACKR1$^+$ endothelial cells expressed *ACKR1*, *IL33*, and *MADCAM1* **(Figure 6D)**, indicating a potential inflammatory role, while FABP5$^+$ endothelial cells expressed higher levels of *FABP5*, *PLVAP*, and *CD36*, resembling a normal endothelium **(Figure 6D)**. Furthermore, this former cluster was mostly derived from normal samples (**Figure 6B-C**). CXCL12$^+$ endothelial cells express *CXCL12*, *SEMA3G*, and *HEY1*, genes linked to neoangiogenesis, migration, and chemoattraction (**Figure 6D**).

Pancreatic stellate cells are resident mesenchymal cells responsible for controlling extracellular matrix production (**Bachem *et al.*, 2006**). Usually, they are quiescent but get activated upon tissue damage (**Jin *et al.*, 2020**). A relevant example of that can be seen by comparing the composition of normal samples against the other conditions (**Figure 6A**). Normal tissue was dominated by endothelial cells, while adjacent tissue showed a significant increase in stellate cells in response to nearby inflammation caused by the growing tumor (**Figure 6B-C**). Both stellate cell clusters had a similar transcription profile; however, one particular gene, *MYH11*, distinguished them **(Figure 6D)**. A recent study of liver fibrosis observed different locations for MYH11$^+$ stellate cells, close to portal vein walls, and RGS5$^+$ stellate cells, confined in hepatic parenchyma, in mouse models (**Dobie *et al.*, 2019**).

CAFs were the most predominant type of stromal cells in the TME. As expected, myCAF were enriched in PDAC compared to adjacent tissue (**Figure 6B**). Although the proportion between PDAC and MET didn't exhibit many differences (except for the increase in Cycling myCAF) there were significantly less stromal cells in MET than in PDAC (**Figure 6B**). myCAF expressed their known signature (*COL11A1*, *COL10A1*, *MMP11*, *POSTN*, *FN1*); alternatively, iCAF were recognized by complement activation (*C3*, *C7*) and inflammatory chemokines (*CCL2*, *CXCL12*) (**Figure 6D; and Supplementary figure 6C-D**). We searched for apCAFs with Elyada geneset

(**Elyada *et al.*, 2019**) but couldn't identify any (**Figure 6G**). Nonetheless, apCAF signature was only enriched in endothelial cells (**Supplementary figure 6A**), which agrees with Wu's work, whom found endothelial cells expressing MHC-II genes in breast cancer (**Wu *et al.*, 2021**). The expression of MHC-II-related genes by endothelial cells reveals potential crosstalk with immune cells.

A topic of high interest about CAFs is to elucidate the origin of their distinct phenotypes. To address this question, we constructed a cell trajectory for CAF and pancreatic stellate cells (**Figure 6E**). Pseudotime analysis revealed a gradual transition of pancreatic stellate cells into myCAF (**Supplementary figure 6B**). This transition was the result of a shift between stellate markers (*ACTA2*, *TAGLN*, *MYH11*, *RGS5*, *NOTCH3*, *ADIRF*) and fibroblast markers (*COL11A1*, *MMP11*, *POSTN*, *FN1*, *FAP*) (**Figure 6F; and Supplementary figure 6E**). We also observed a few cells positive for both myCAF and iCAF scores (**Figure 6G**). A recent preprint detected CAFs double positive for iCAF and myCAF reinforcing the plasticity of these cells (**Kinny-Köster *et al.*, 2022**). These results indicate a high diversity of stromal cells present in the TME.

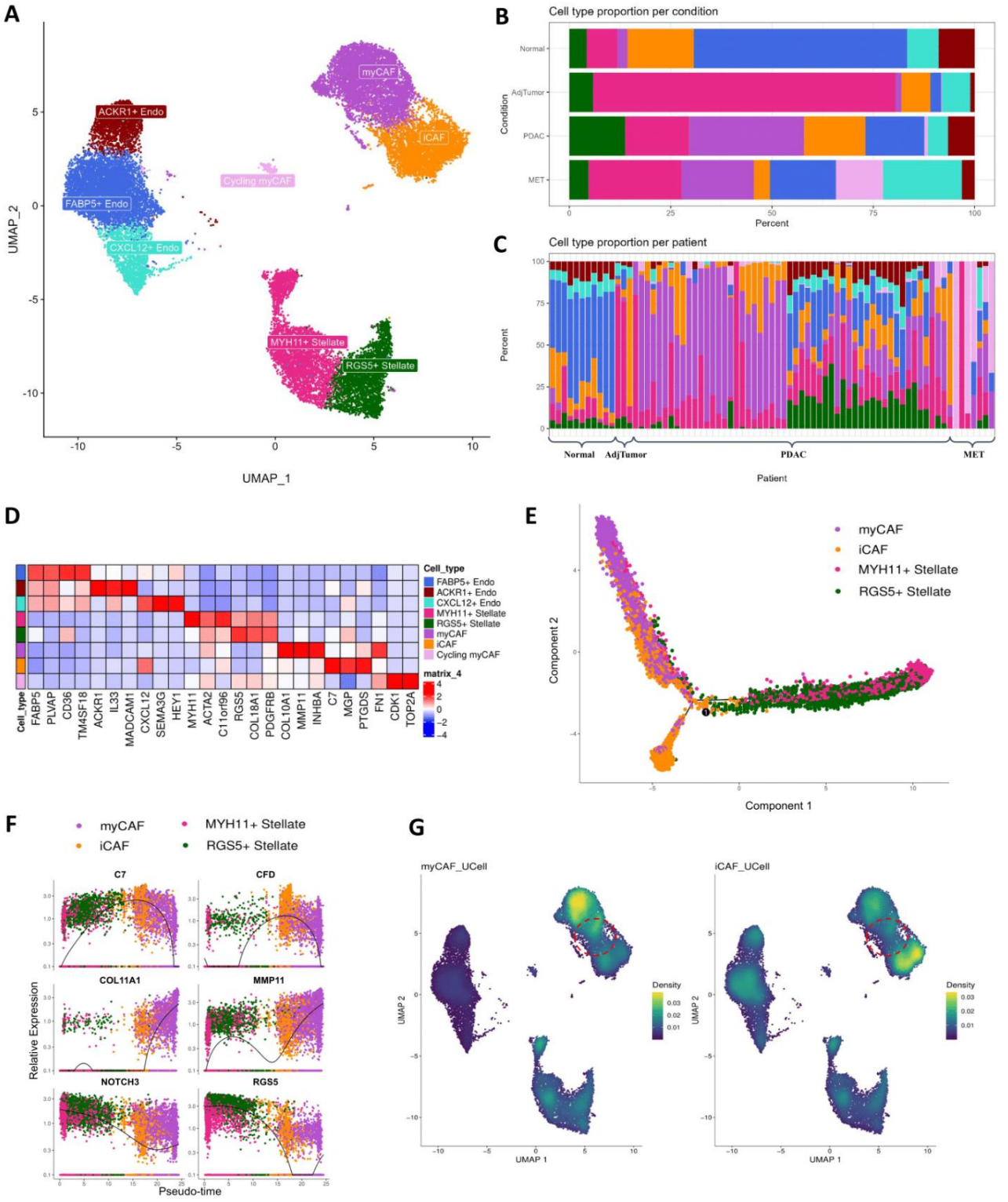



**Figure 6 - Characterization of stromal cells in PDAC-associated lesions. A**) Reclustered stromal cells (n=27.648). **B**) Cell type quantification across the four different conditions. **C**) Cell type quantification across individuals. **D**) Mean normalized expression of markers for each cluster. **E**) Cell trajectory analysis for fibroblasts and stellate cells. **F**) Expression of genes that change as a function of pseudotime for fibroblasts and stellate cells. **G**) Density plot for myCAF and iCAF signatures score.

### 3.5 - CAFs command extracellular signaling in the tumor microenvironment

Finally, we sought to characterize the cellular crosstalk within the TME and compare its interactions across conditions driving tumor progression. To achieve this, we used *CellChat*, an R package that analyze intercellular communications from scRNA-seq data. Our input included all the previously annotated clusters. Clusters with less than 10 cells were filtered out before interaction inference.

Among the three conditions, stromal cells (CAFs, pancreatic stellate cells, and endothelial cells) exhibited a higher number of interactions and higher strength compared to epithelial cells and immune cells (**Figure 7A; and Supplementary figure 8A-C**). Immune cells, especially the CD8 cells, were strongly modulated, receiving signals from multiple cell types while sending only a few weak signals in both primary PDAC and MET (**Figure 7A; and Supplementary figure 8A-C**). In contrast, CAFs (especially myCAF) accounted for the most signals sent and stronger force of interaction in PDAC and MET (**Figure 7A; and Supplementary figure 8A-C**). Therefore, we could assign CD8 cells as a hub of incoming signals while CAFs command outgoing signals. In adjacent tissue, there was a balance between incoming and outgoing signals from the CD8 cells compared to malignancy, reflecting a more active role, although the incoming strength was slightly higher than the outgoing (**Figure 7A; and Supplementary figure 8A-C**).

Then, we assessed the different signaling pathways enriched in each biological condition. MHC-I and LCK pathways had a higher score in adjacent tissue and metastasis compared to PDAC (**Supplementary figure 7A-B**). This might be explained by the modulation that CD8 cells suffer in PDAC, resulting in a lower engagement of anti-tumor immunity (**Ene-Obong *et al.*, 2013; Zhu *et al.*, 2014; Carstens *et al., 2017*; Candido *et al.*, 2018; Karamitopoulou, 2019**). Immune checkpoint-related pathways presented higher interaction in both malignant tissues than in adjacent tissue. CAFs played a major role in collagen and fibronectin pathways, which are linked to tumor progression (**Winkler *et al.*, 2020**). However, depletion of α-SMA (alpha-smooth muscle actin) or type I collagen in myCAFs promoted tumor progression suggesting that a fraction of myCAFs harbor antitumor features (**Özdemir *et al.*, 2014; Chen *et al.*, 2021**). These pathways were strongly related to PDAC samples (**Supplementary figure 7A-B**). Immune cells - dendritic cells, monocytes, and macrophages - heavily contributed to galectin and SPP1 pathways which are related to cancer cell survival, immune checkpoint activation, response to hypoxia, and angiogenesis (**Zhang *et al.*, 2020; Cheng *et al.*, 2021**). Again, both pathways showed higher interaction in PDAC (**Supplementary figure 7A-B**).

Lastly, we searched for ligand-receptor pairs that were overexpressed. The pair LGALS9-HAVCR2 is known for blocking antitumor immunity in lymphocytes (**Wolf *et al.*, 2020**). A similar

effect is also found in dendritic cells, thus carrying a potential target for immunotherapy (**Dixon *et al.*, 2021**) (**Figure 7B**). This pair was overexpressed in the malignant tissue. Previously, we identified that memory CD8 cells were enriched adjacent tissue, but not in malignant tissue. The expression of the receptor, *CXCR6*, and its ligand, *CXCL16*, may be responsible for sustaining the memory state in CD8 cells (**Muthuswamy *et al.*, 2021**) We compared this pair level and found that it is higher in adjacent tissue, especially *CXCR6*, justifying the contrast in the proportion of this cell state (**Figure 7B**). Another pair related to the CXCL pathway, CXCL12-CXCR4, is recognized for its role in desmoplasia reaction and mitigating cytotoxic response, and trapping CD8 cells in the stroma (**Seo *et al.*, 2019**). Once again, this pair showed high levels in the malignant tissue (**Figure 7B**).

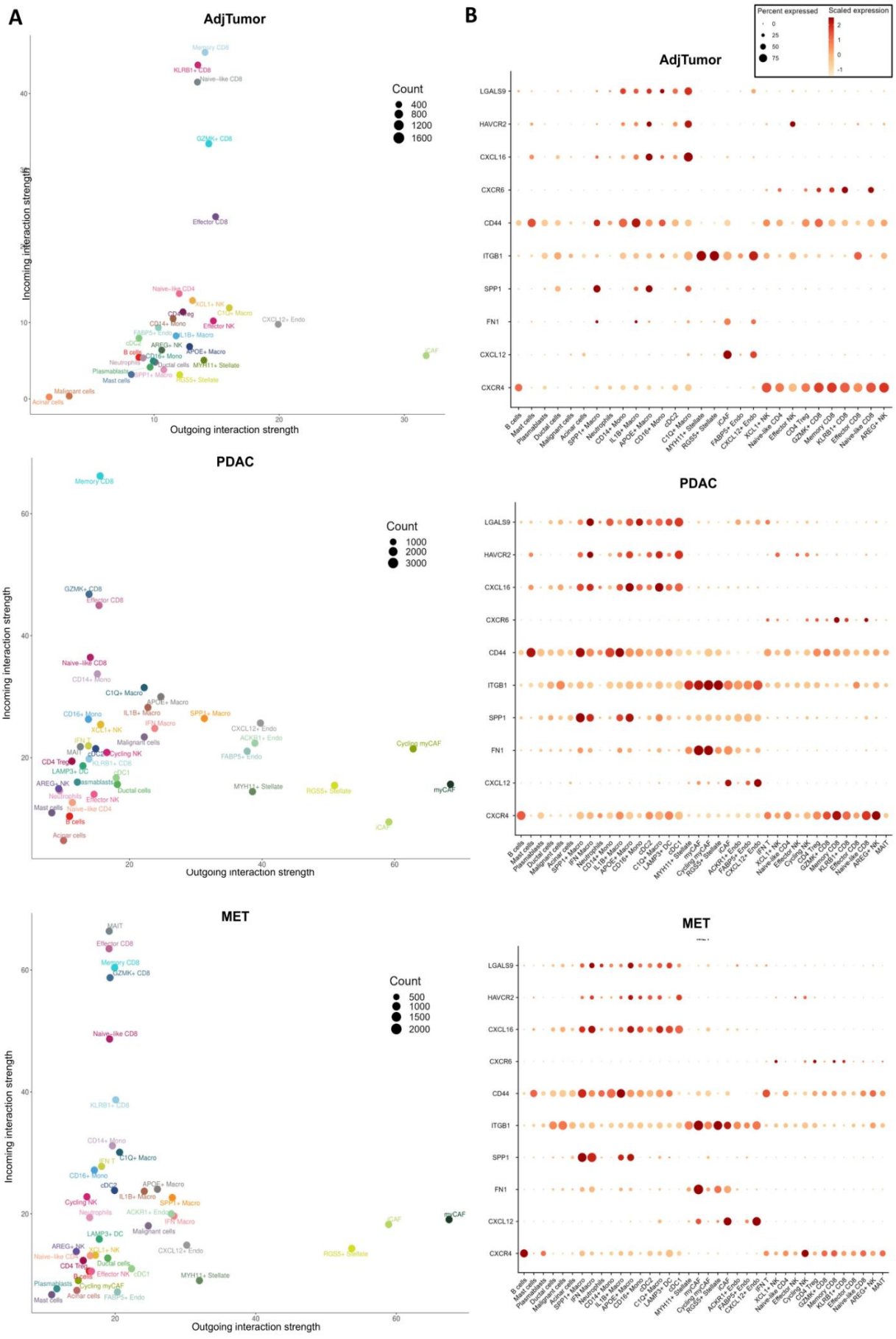

A
AdjTumor
Incoming interaction strength
Outgoing interaction strength
Count
400
800
1200
1600
PDAC
Count
1000
2000
3000
MET
Count
500
1000
1500
2000
B
AdjTumor
Percent expressed
Scaled expression
LGALS9
HAVCR2
CXCL16
CXCR6
CD44
ITGB1
SPP1
FN1
CXCL12
CXCR4
PDAC
MET

**Figure 7** – **Inferred intercellular communication in PDAC-associated lesions. A**) Scatter plot for incoming (y-axis) and outgoing (x-axis) interactions strength of each cluster. **B**) Dotplot with normalized expression values for ligand-receptor pairs.

## 4. Discussion

In this study, we performed scRNA-seq integration from multiple datasets to build a detailed characterization of cell composition, cell trajectories, and cell-cell interactions for distinct biological conditions that recapitulates different moments of pancreatic carcinogenesis. Our approach differed from recent works that only integrated normal and PDAC samples (**Chijimatsu *et al.*, 2022; Kinny-Köster *et al.*, 2022**). Deconvolution of the TME identified a highly heterogeneous composition in PDAC with 2 distinct groups: one enriched in fibroblasts/stellate cells and low infiltration of lymphoid cells while the other was enriched in lymphoid cells and poor in fibroblasts/stellate cells. Adjacent tissue was dominated by high infiltration of immune cells diverging from the homeostasis identified in the normal pancreatic tissue. Moreover, memory and effector T cells were higher in adjacent tissue compared to PDAC. Therefore, we should carefully use adjacent tissue as a reference for any comparison because these differences might be caused by host response or promoted by the tumor cells to avoid cytotoxic and memory T cells.

Myeloid cells are one of the main drivers of the tumor-supporting microenvironment found in PDAC. Macrophages are highly heterogeneous and express high levels of *APOE*. We identified 3 major subpopulations of macrophages, $APOE^+$ macro, $SPP1^+$ macro, and $C1Q^+$ macro, that have already been described in pancreatic cancer, however, their respective roles are not fully understood (**Cheng *et al.*, 2021; Revel *et al.*, 2022; Werba *et al.*, 2022**). APOE+ macro cluster showed high levels of *SPP1* and complement genes, suggesting a potential common origin for both clusters, which was later confirmed in our cell trajectory analysis. Moreover, we also observed a transition from $CD14^+$ monocytes to early activated macrophages, IL1B+ macro, showing that monocytes can infiltrate and later differentiate into macrophages within the PDAC TME. Strikingly, there was a subgroup of cells within the $CD14^+$ cluster that coexpressed *CD163* and MHC-II pathway genes, reflecting an intermediate state. Dendritic cells are sparse in PDAC and were the minor cell type found within the myeloid cells. Besides, cDC2s were the most frequent cell type contributing to an immunosuppressive environment, whereas cDC1s, which harbor an anti-tumoral response, were less frequent. The small cluster of $LAMP3^+$ DCs has been previously described as a mature dendritic cell involved with antigen presentation and is mainly found in tertiary lymphoid structures (TLS) (**Sautès-Fridman *et al.*, 2019**). However, we detected the expression of immune checkpoint markers, *CD274* and *IDO1,* and chemokines that recruit regulatory T cells, *CCL17*, *CCL19,* and *CCL22*, in $LAMP3^+$ DC cells, implying a potential regulatory role to them in the TME. Likewise, a recent study identified

an increase of LAMP3$^+$ DCs in TLS together with high infiltration of FOXP3$^+$ Treg cells in TME from PDAC compared to low-grade IPMN (**Roth *et al.*, 2020**). Finally, in our trajectory analysis, we found that LAMP3$^+$ DCs were derived from cDC2 cells, but not from cDC1 cells as usual for other malignancies. Furthermore, this alternative cell of origin could explain the controversial impact on the prognosis of multiple neoplasias - good for triple-negative breast cancer and esophageal squamous cell carcinoma; bad for uterine cervical cancer and nasopharyngeal carcinoma (**Kanao *et al.*, 2005; de Mingo Pulido *et al.*, 2018; Nishimura *et al.*, 2019; Liu *et al.*, 2021**).

CAFs are more than bystanders in the TME and exert multiple protumoral roles (**Sahai *et al.*, 2020**); however, a few studies revealed a potential anti-tumoral for specific subpopulations of CAF (**Özdemir *et al.*, 2014; Chen *et al.*, 2021**). Furthermore, CAFs have a dynamic and heterogeneous transcription profile and can arise from different cells of origin. CAFs can be derived especially from pancreatic stellate cells (**Öhlund *et al.*, 2017; Biffi & Tuveson, 2020; Sahai *et al.*, 2020**). A recent study unraveled that myCAFs derived from stellate cells present a distinct transcriptomic profile compared to myCAFs derived from other sources (**Helms *et al.*, 2022**). Here, we reported a transition from stellate cells into myCAF which comes in agreement with this result. We also identified a few iCAF transitioning to myCAF. This interchange between iCAF and myCAF is well characterized both *in vitro* and *in vivo* (**Öhlund *et al.*, 2017; Biffi *et al.*, 2019; Steele *et al.*, 2021**).

The complexity of the TME, a hallmark of PDAC, is determined by cell composition and cell-cell interactions. Our results revealed cell signaling hierarchy within the TME. Stromal cells, especially CAFs, sent multiple signals which lead to an intricate interaction network with malignant cells and immune cells. This pattern was also observed in PDAC mouse models (**Velez-Delgado *et al.*, 2021**). myCAFs overexpressed different types of collagen and extracellular matrix-related genes that contribute to the invasiveness of malignant cells. Moreover, this dense extracellular matrix could be a barrier to lymphocyte infiltration (**Ene-Obong *et al.*, 2013; Seo *et al.*, 2019**). In contrast, CD8$^+$ T cells received a lot of signals suffering modulation from different cell types. Most of the pathways enriched in CD8$^+$ T cells were related to antigen presentation and lymphocyte activation. Furthermore, these pathways showed enrichment in the adjacent tissue samples rather than malignancies. PDAC is still refractory to the main immune checkpoint inhibitors due to the low expression of PDL1 (*CD274*) and CTLA4 (**Fan *et al.*, 2020**). Our analysis later confirmed this as the TIGIT pathway was the only immune checkpoint pathway enriched in lymphocytes and NK cells. We also found ligand-receptor pairs that could justify the differences in the TME composition between adjacent tissue and malignant tissue. Memory CD8$^+$ T cells are recognized by *CXCR6* expression which is higher in the adjacent tissue samples compared to PDAC. *In vivo* analysis showed that the recruitment of T cells in the TME was dependent on *CXCR6* expression by T cells and

*CXCL16* expression by malignant or myeloid cells (**Lesch *et al.*, 2021**). Metastatic lesions showed higher expression of *SPP1* which can bind to *CD44* and *ITGB1* leading to enhanced cancer stemness and neoangiogenesis (**Nallasamy *et al.*, 2021**). In fact, $SPP1^{+}$ macrophages were enriched in metastasis. Strikingly, we detected high expression of *HAVCR2* (TIM-3) in myeloid cells (especially dendritic cells), but not in lymphoid cells. *HAVCR2* is a regulator of immune response and has potential value for immune checkpoint blockade (**Wolf *et al.*, 2020**). Immunotherapy mainly focuses on lymphoid cells, however, a recent study revealed that *HAVCR2* blockade on dendritic cells exhibited a stronger effect in antitumor immunity than T cells (**Dixon *et al.*, 2021**).

The results presented in this work should be taken carefully as they may not be the full representation of PDAC. Indeed, differences in sequencing depth might introduce artifacts even when batch correction from multiple data integration is performed. Furthermore, clinical data was not publicly available for all datasets. Single-cell RNA-seq is the gold standard for cell type/state identification, however, we lose spatial resolution which is really important in the context of cancer. Therefore, our cell-cell interaction prediction might not correspond to the "real-world biology" of PDAC. As the use of spatial transcriptomics technology continues to increase it will be very helpful to unravel the full complexity of the TME in this deadly disease (**Moncada *et al.*, 2020; Hwang *et al.*, 2022; Zhou *et al.*, 2022**).

Collectively, our work provides a refined characterization of the TME composition in distinct biological conditions of PDAC and an in-depth view of the intricate cell-cell interactions within its TME. Moreover, the L-R pair interactions highlighted here can be useful for personalized medicine turning PDAC into an immune hot tumor.

## 5. Conclusion

Here we found that the TME composition varies between distinct conditions. Moreover, the TME plays a role in the polarization and differentiation of immune and mesenchymal cells. CAFs and stellate cells are the major sources of outgoing signals shaping the TME towards a fibrotic environment. High expression of specific L-R pairs can explain the differences in cell composition across conditions. Therefore, we could exploit particular interactions that may increase lymphocyte infiltration and reactivate antitumor immunity combined with chemotherapy or immunotherapy.

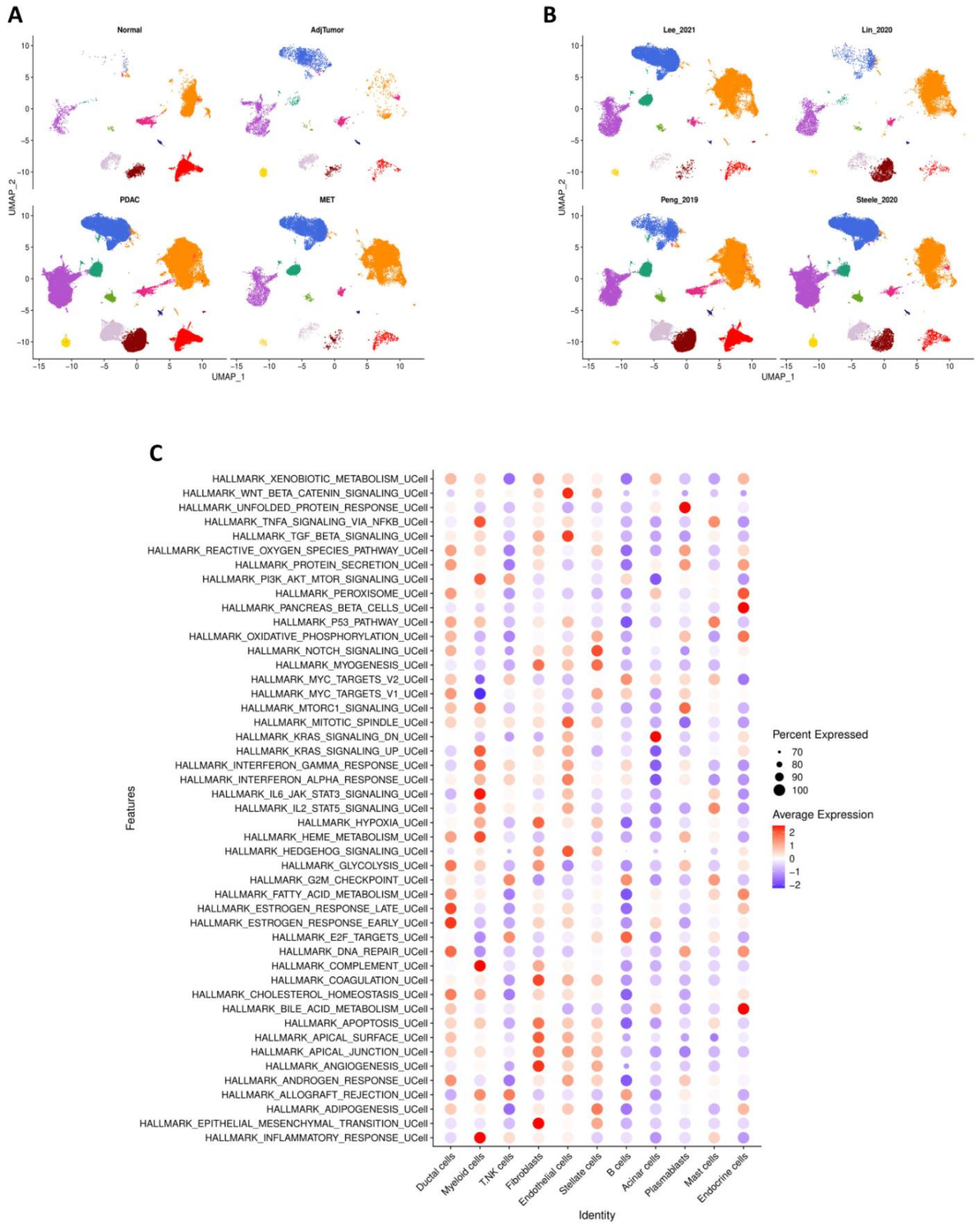
## Acknowledgments

This study was financed in part by the Coordenação de Aperfeiçoamento de Pessoal de Nível Superior - Brasil (CAPES) - Finance Code 001. Funding agencies had no role in the study design, data collection and analysis, decision to publish, or preparation of the manuscript.

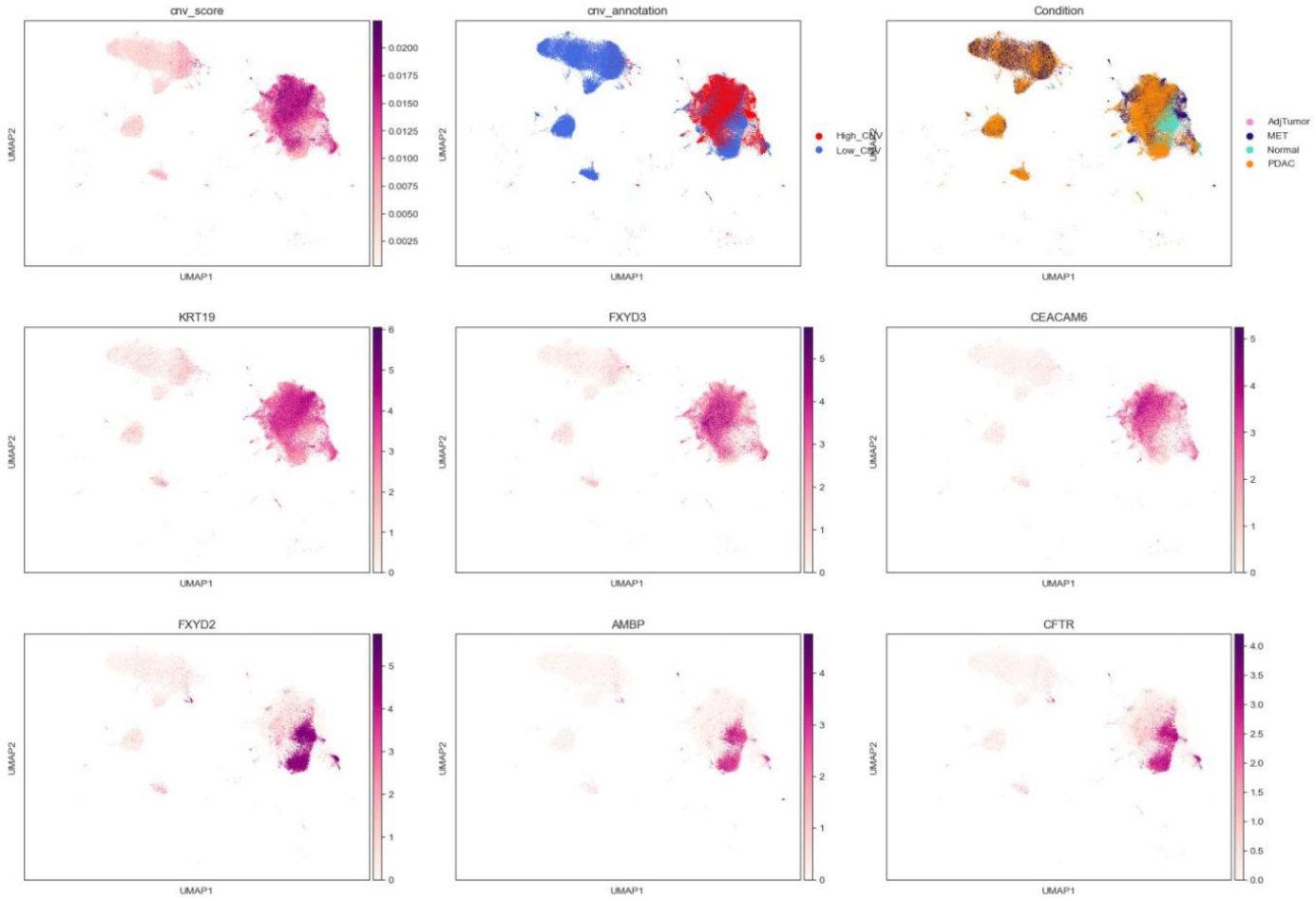
## Conflict of Interest

No conflict of interest.

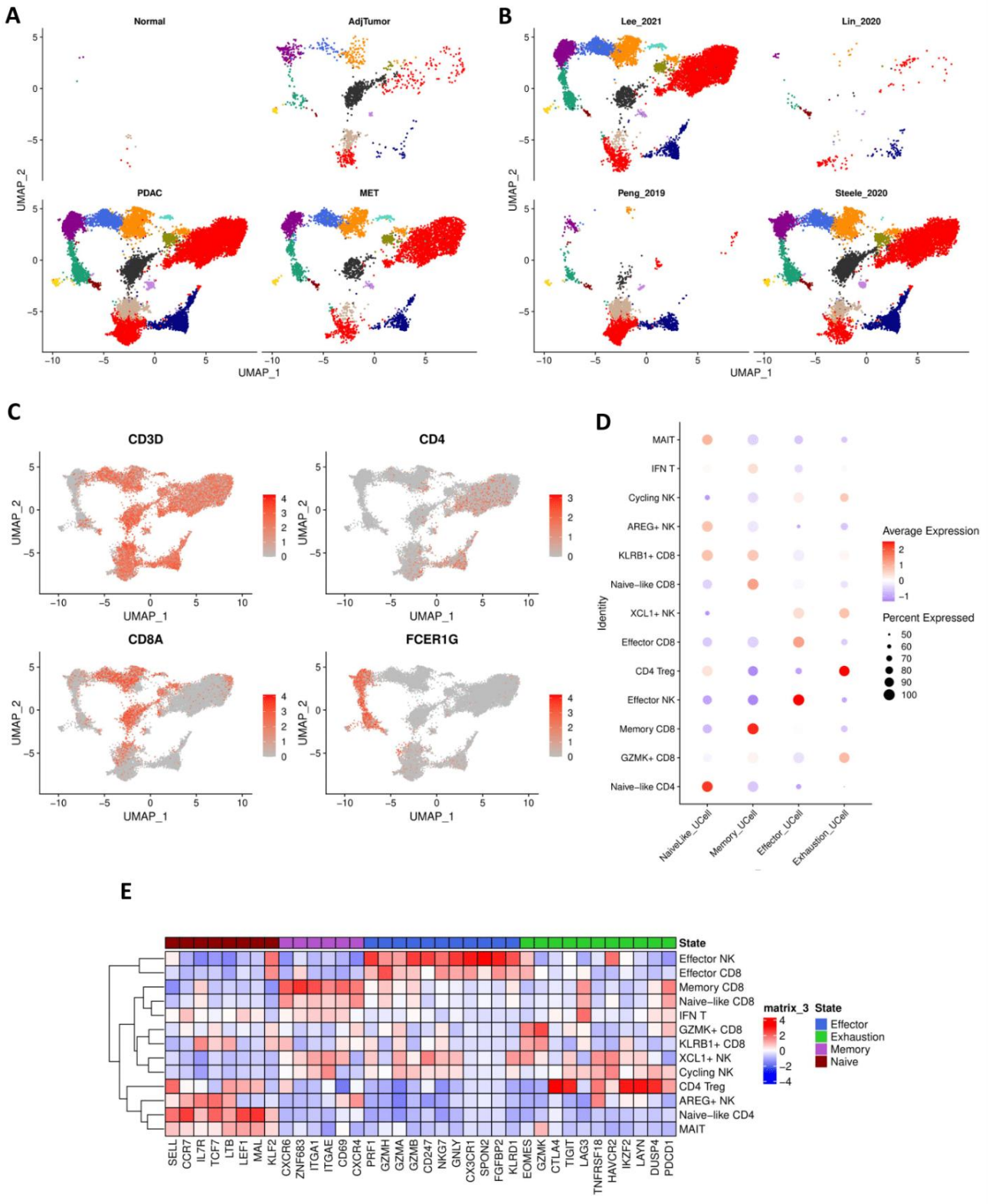
## Supplementary figures



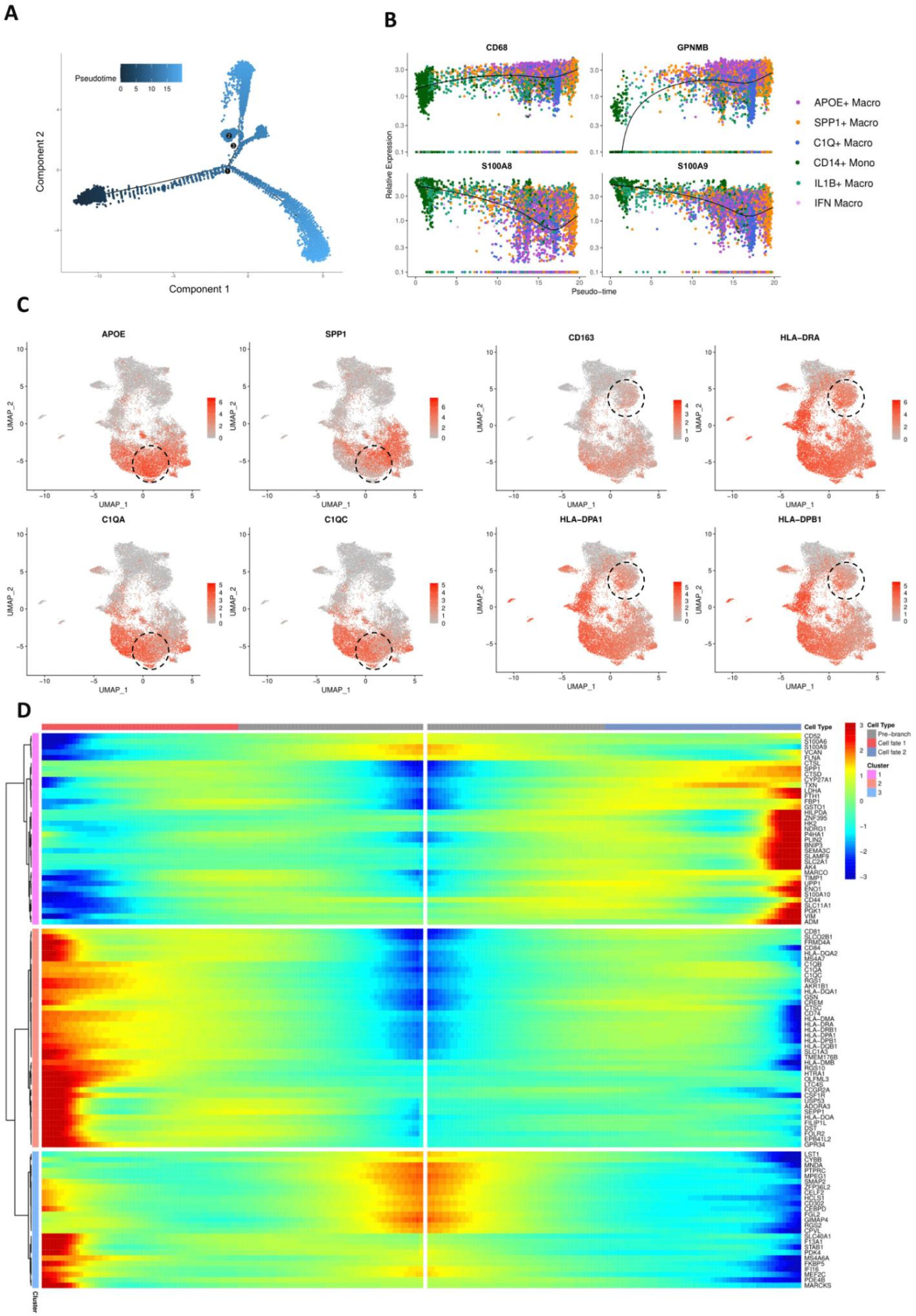

**Supplementary figure 1** - **A**) UMAP of 137,699 cells derived from data integration split by condition. **B**) UMAP of 137,699 cells derived from data integration split by dataset. **C**) Pathway enrichment score with UCell. Hallmark gene sets were obtained from MSigDB. Signature scores were calculated for each cell.



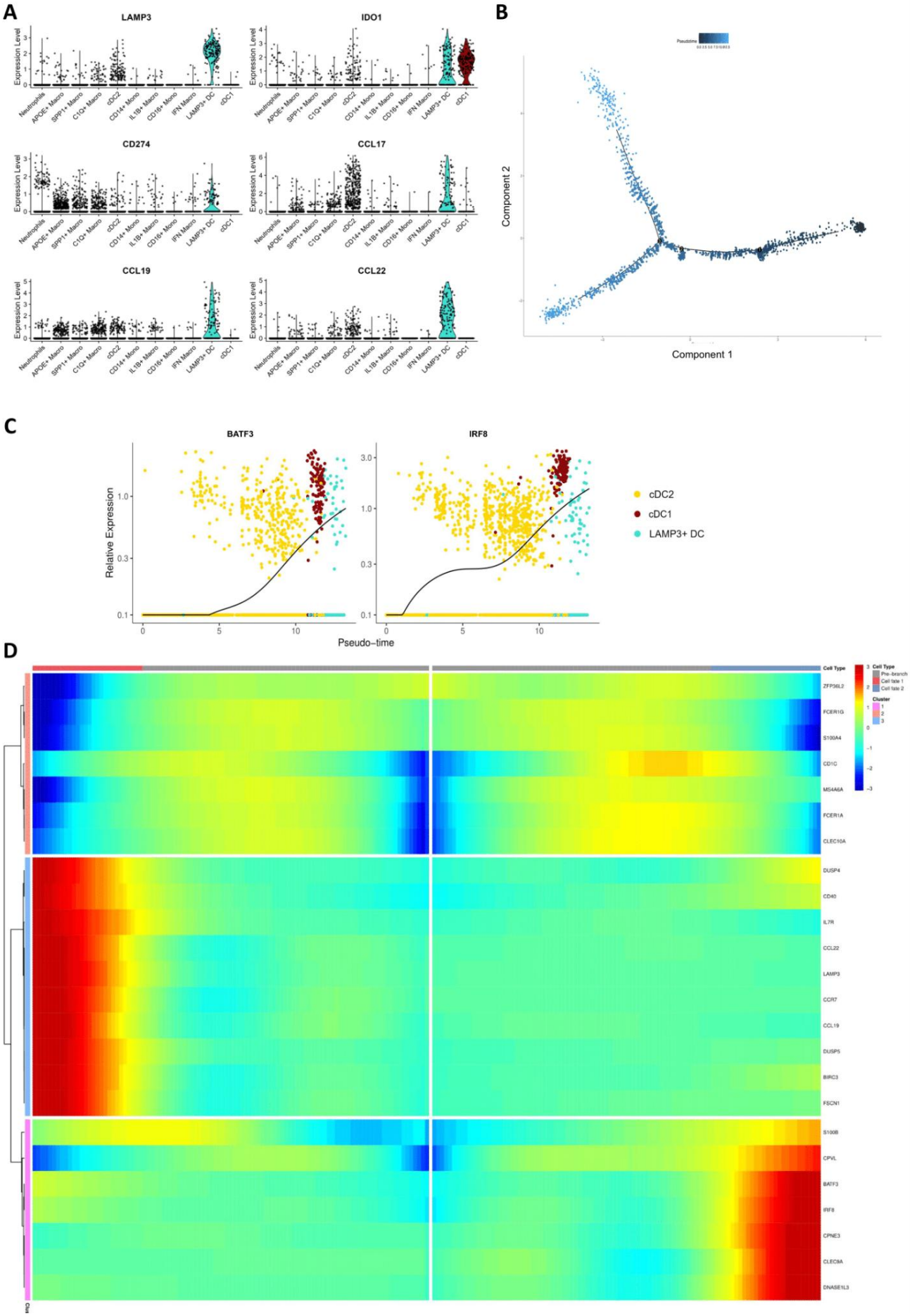

**Supplementary figure 2** - Feature plot with log-normalized values.



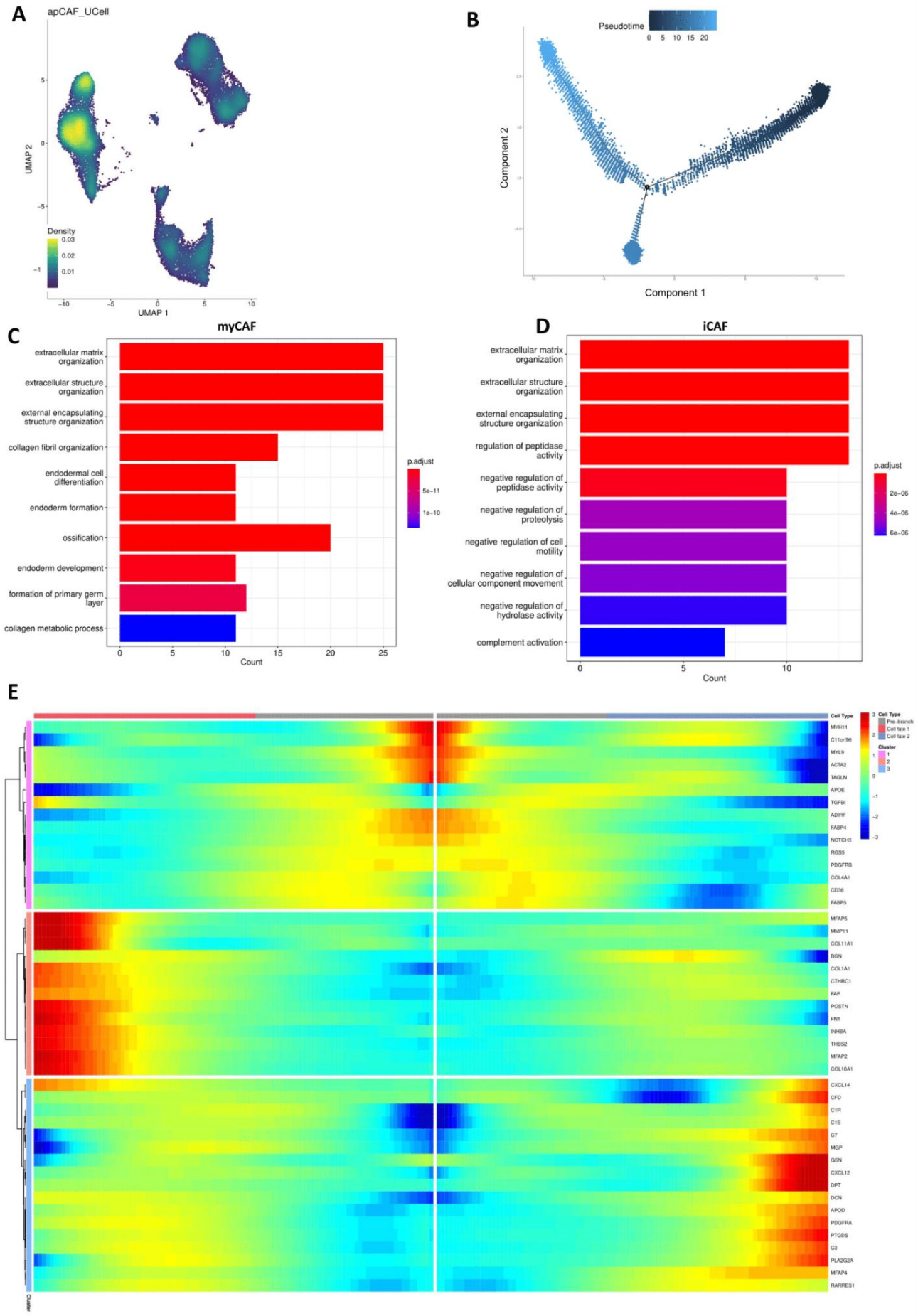

**Supplementary figure 3 - A**) UMAP of 24,124 cells derived from data integration split by condition. **B**) UMAP of 24,124 cells derived from data integration split by dataset. **C**) Feature plot with log-normalized values for *CD3D*, *CD4*, *CD8A*, and *FCER1G*. **D**) Average expression of the signature scores (Naive-like, Effector, Memory, and Exhaustion) in the lymphoid clusters identified. **E**) Heatmap for the enriched genes related to the distinct cell states. Average expression values.


A
Pseudotime
0 5 10 15
Component 2
Component 1
B
CD68
GPNMB
S100A8
S100A9
Relative Expression
Pseudo−time
APOE+ Macro
SPP1+ Macro
C1Q+ Macro
CD14+ Mono
IL1B+ Macro
IFN Macro
C
APOE
SPP1
CD163
HLA−DRA
C1QA
C1QC
HLA−DPA1
HLA−DPB1
UMAP_1
UMAP_2
D
Cell Type
Pre−branch
Cell fate 1
Cell fate 2
Cluster
Cluster

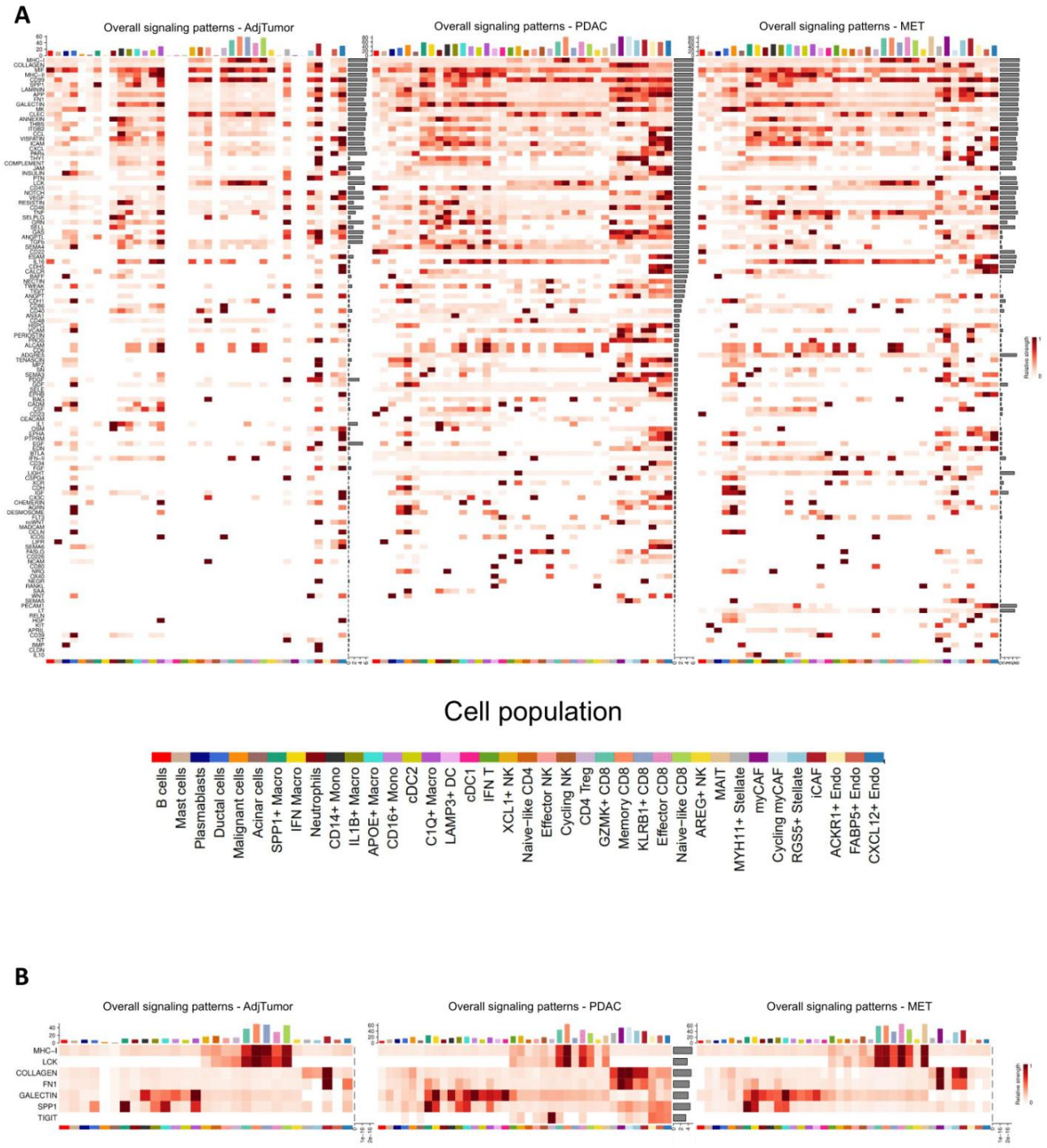
**Supplementary figure 4 - A**) Cell trajectory analysis for monocytes and macrophages colored by pseudotime. Navy blue = beginning of the trajectory; Royal Blue = end of the trajectory. **B**) Expression of genes that change as function of pseudotime for monocytes and macrophages. **C**) Feature plot with log-normalized expression for *APOE*, *SPP1*, *C1QA*, *C1QC*. **D**) Pseudotime heatmap with the genes that change as a function of pseudotime identified in branch 1. Gray bar = all cells before branching; Red = transition towards $C1Q^{+}$ Macro; Blue = transition towards $SPP1^{+}$ Macro.


A
LAMP3
IDO1
CD274
CCL17
CCL19
CCL22
Expression Level
Neutrophils
APOE+ Macro
SPP1+ Macro
C1Q+ Macro
cDC2
CD14+ Mono
IL1B+ Macro
CD16+ Mono
IFN Macro
LAMP3+ DC
cDC1
B
Component 1
Component 2
C
BATF3
IRF8
Relative Expression
Pseudo−time
cDC2
cDC1
LAMP3+ DC
D
Cell Type
Pre−branch
Cell fate 1
Cell fate 2
Cluster
ZFP36L2
FCER1G
S100A4
CD1C
MS4A6A
FCER1A
CLEC10A
DUSP4
CD40
IL7R
CCL22
LAMP3
CCR7
CCL19
DUSP5
BIRC3
FSCN1
S100B
CPVL
BATF3
IRF8
CPNE3
CLEC9A
DNASE1L3

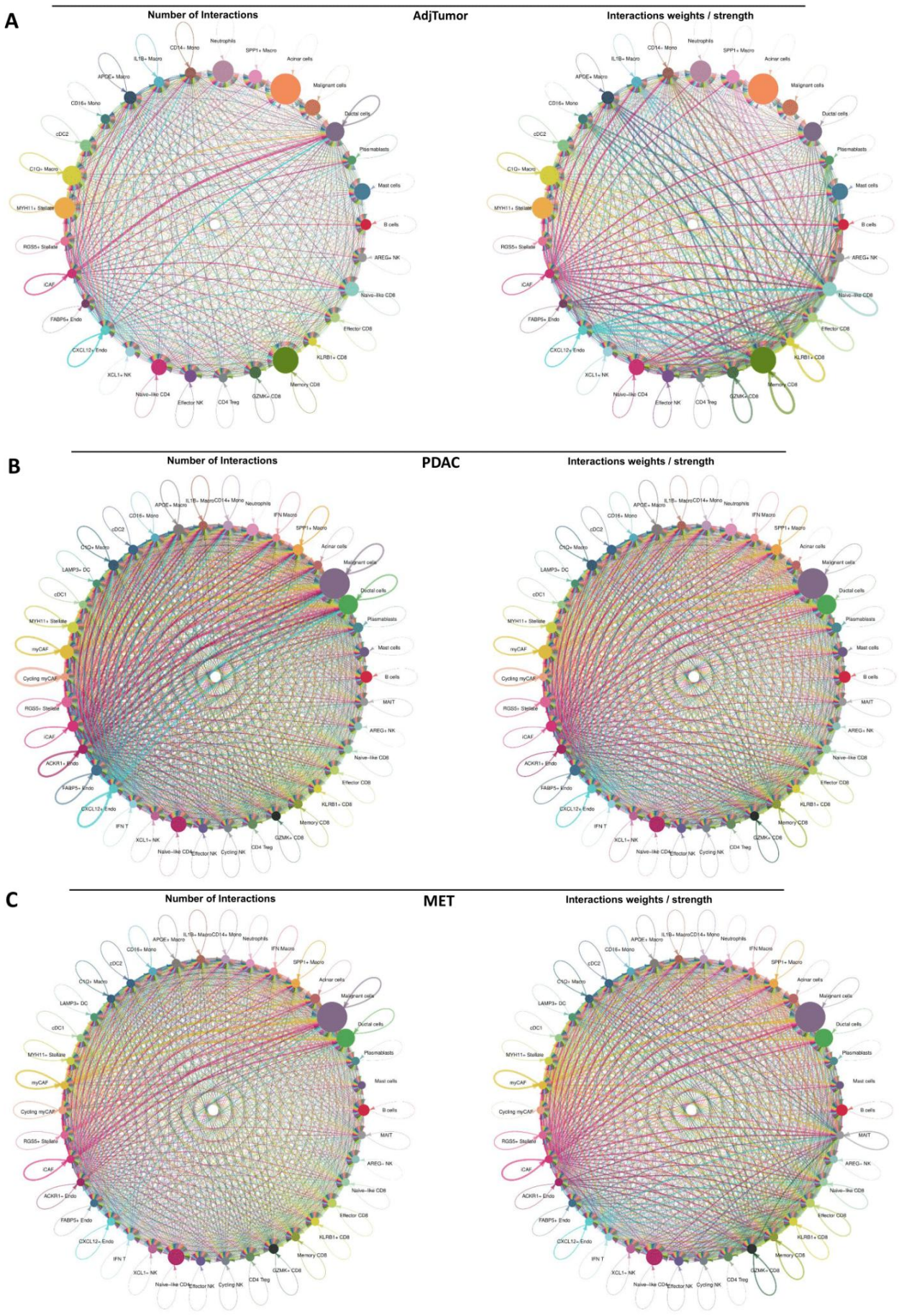
**Supplementary figure 5 - A)** Violin plot of immunosuppressive markers expressed by LAMP3$^{+}$ DC. Each dot represents a single cell and values of expression are normalized. **B**) Cell trajectory analysis for dendritic cells colored by pseudotime. Navy blue = beginning of the trajectory; Royal Blue = end of the trajectory. **C**) Expression of genes that change as a function of pseudotime for dendritic cells. **D**) Pseudotime heatmap with the genes that change as a function of pseudotime identified in branch 3. Gray bar = all cells before branching; Red = transition towards LAMP3$^{+}$ DC; Blue = transition towards cDC1.


A
apCAF_UCell
UMAP 2
UMAP 1
Density
0.03
0.02
0.01
B
Pseudotime
0 5 10 15 20
Component 2
Component 1
C
myCAF
extracellular matrix organization
extracellular structure organization
external encapsulating structure organization
collagen fibril organization
endodermal cell differentiation
endoderm formation
ossification
endoderm development
formation of primary germ layer
collagen metabolic process
p.adjust
5e-11
1e-10
Count
D
iCAF
extracellular matrix organization
extracellular structure organization
external encapsulating structure organization
regulation of peptidase activity
negative regulation of peptidase activity
negative regulation of proteolysis
negative regulation of cell motility
negative regulation of cellular component movement
negative regulation of hydrolase activity
complement activation
p.adjust
2e-06
4e-06
6e-06
Count
E
Cell Type
Pre-branch
Cell fate 1
Cell fate 2
Cluster
MYH11
C11orf96
MYL9
ACTA2
TAGLN
APOE
TGFBI
ADIRF
FABP4
NOTCH3
RGS5
PDGFRB
COL4A1
CD36
FABP5
MFAP5
MMP11
COL11A1
BGN
COL1A1
CTHRC1
FAP
POSTN
FN1
INHBA
THBS2
MFAP2
COL10A1
CXCL14
CFD
C1R
C1S
C7
MGP
GSN
CXCL12
DPT
DCN
APOD
PDGFRA
PTGDS
C3
PLA2G2A
MFAP4
RARRES1
Cluster

**Supplementary figure 6 - A)** Density plot for apCAF signature score. **B**) Cell trajectory analysis for fibroblasts and stellate cells colored by pseudotime. Navy blue = beginning of the trajectory; Royal Blue = end of the trajectory. **C**) Gene-ontology pathway enrichment for myCAF. **D**) Gene-ontology pathway enrichment for iCAF. **E**) Pseudotime heatmap with the genes that change as a function of pseudotime identified in branch 1. Gray bar = all cells before branching; Red = transition towards myCAF; Blue = transition towards iCAF.




**Supplementary figure 7** - **A**) Heatmap of the overall signaling pattern for all curated pathways. **B**) Heatmap of the overall signaling pattern for filtered pathways.




**Supplementary figure 8** - **A**) Cell-cell communication network for AdjTumor. **B**) Cell-cell communication network for PDAC. **C**) Cell-cell communication network for MET.

## Supplementary table

| Cluster | Pathways | p-value adjusted |
|---|---|---|
| SPP1$^{+}$ macro | response to hypoxia | 1.246216e-13 |
| SPP1$^{+}$ macro | response to decreased oxygen levels | 2.004619e-13 |
| SPP1$^{+}$ macro | response to oxygen levels | 8.198653e-13 |
| SPP1$^{+}$ macro | ADP metabolic process | 8.348193e-12 |
| SPP1$^{+}$ macro | nucleoside diphosphate phosphorylation | 2.469342e-11 |
| SPP1$^{+}$ macro | glycolytic process | 2.469342e-11 |
| SPP1$^{+}$ macro | ATP generation from ADP | 2.469342e-11 |
| SPP1$^{+}$ macro | nucleotide phosphorylation | 2.469342e-11 |
| SPP1$^{+}$ macro | purine nucleoside diphosphate metabolic process | 2.665076e-11 |
| SPP1$^{+}$ macro | purine ribonucleoside diphosphate metabolic process | 2.665076e-11 |
| C1Q$^{+}$ macro | antigen processing and presentation of peptide antigen via MHC class II | 4.710771e-21 |
| C1Q$^{+}$ macro | antigen processing and presentation of peptide or polysaccharide antigen via MHC class II | 1.857672e-17 |
| C1Q$^{+}$ macro | MHC class II protein complex assembly | 2.699294e-17 |
| C1Q$^{+}$ macro | peptide antigen assembly with MHC class II protein complex | 2.699294e-17 |
| C1Q$^{+}$ macro | antigen processing and presentation of exogenous peptide antigen | 3.198908e-17 |
| C1Q$^{+}$ macro | MHC protein complex assembly | 2.61291e-16 |
| C1Q$^{+}$ macro | antigen processing and presentation of exogenous peptide antigen | 8.542529e-16 |
| C1Q$^{+}$ macro | antigen processing and presentation of exogenous antigen | 1.851008e-14 |
| C1Q$^{+}$ macro | antigen processing and presentation of peptide antigen | 2.368437e-14 |
| CD14$^{+}$ mono | cytoplasmic translation | 5.919044e-18 |
| CD14$^{+}$ mono | interleukin-1 production | 5.842761e-08 |
| CD14$^{+}$ mono | regulation of interleukin-1 production | 5.842761e-08 |
| CD14$^{+}$ mono | interleukin-1 beta production | 8.437112e-08 |

| | | |
|---|---|---|
| CD14$^+$ mono | regulation of interleukin-1 beta production | 8.437112e-08 |
| CD14$^+$ mono | regulation of inflammatory response | 3.312218e-07 |
| CD14$^+$ mono | formation of cytoplasmic translation initiation complex | 9.535257e-07 |
| CD14$^+$ mono | positive regulation of cytokine production | 9.535257e-07 |
| CD14$^+$ mono | response to lipopolysaccharide | 1.667001e-06 |
| CD14$^+$ mono | positive regulation of NF-kappaB transcription factor activity | 1.800147e-06 |
| IL1B$^+$ macro | cytokine-mediated signaling pathway | 7.220398e-09 |
| IL1B$^+$ macro | leukocyte chemotaxis | 1.523366e-08 |
| IL1B$^+$ macro | chemokine-mediated signaling pathway | 2.176879e-08 |
| IL1B$^+$ macro | granulocyte chemotaxis | 2.190347e-08 |
| IL1B$^+$ macro | cell chemotaxis | 2.190347e-08 |
| IL1B$^+$ macro | leukocyte migration | 2.190347e-08 |
| IL1B$^+$ macro | response to chemokine | 2.190347e-08 |
| IL1B$^+$ macro | cellular response to chemokine | 2.190347e-08 |
| IL1B$^+$ macro | myeloid leukocyte migration | 2.805453e-08 |
| IL1B$^+$ macro | neutrophil chemotaxis | 3.205336e-08 |

**Supplementary table** - Functional enrichment analysis with Gene-Ontology (GO: Biological Processes) for myeloid subpopulations (SPP1$^+$ macro, C1Q$^+$ macro, CD14$^+$ mono, and IL1B$^+$ macro).

**REFERENCES**

1- Kleeff J, Korc M, Apte M, et al. **Pancreatic cancer**. *Nat Rev Dis Primers*. 2016;2:16022. Published 2016 Apr 21. doi:10.1038/nrdp.2016.22

2- Park W, Chawla A, O'Reilly EM. **Pancreatic Cancer: A Review** [published correction appears in JAMA. 2021 Nov 23;326(20):2081]. *JAMA*. 2021;326(9):851-862. doi:10.1001/jama.2021.13027

3- Siegel RL, Miller KD, Fuchs HE, Jemal A. **Cancer Statistics, 2021** [published correction appears in CA Cancer J Clin. 2021 Jul;71(4):359]. *CA Cancer J Clin*. 2021;71(1):7-33. doi:10.3322/caac.21654

4- Ho WJ, Jaffee EM, Zheng L. **The tumour microenvironment in pancreatic cancer - clinical challenges and opportunities**. *Nat Rev Clin Oncol*. 2020;17(9):527-540. doi:10.1038/s41571-020-0363-5

5- Roth S, Zamzow K, Gaida MM, et al. **Evolution of the immune landscape during progression of pancreatic intraductal papillary mucinous neoplasms to invasive cancer**. *EBioMedicine*. 2020;54:102714. doi:10.1016/j.ebiom.2020.102714

6- Grünwald BT, Devisme A, Andrieux G, et al. **Spatially confined sub-tumor microenvironments in pancreatic cancer**. *Cell*. 2021;184(22):5577-5592.e18. doi:10.1016/j.cell.2021.09.022

7- Schlesinger Y, Yosefov-Levi O, Kolodkin-Gal D, et al. **Single-cell transcriptomes of pancreatic preinvasive lesions and cancer reveal acinar metaplastic cells' heterogeneity**. *Nat Commun*. 2020;11(1):4516. Published 2020 Sep 9. doi:10.1038/s41467-020-18207-z

8- Lin W, Noel P, Borazanci EH, et al. **Single-cell transcriptome analysis of tumor and stromal compartments of pancreatic ductal adenocarcinoma primary tumors and metastatic lesions**. *Genome Med*. 2020;12(1):80. Published 2020 Sep 29. doi:10.1186/s13073-020-00776-9

9- Lee JJ, Bernard V, Semaan A, et al. **Elucidation of Tumor-Stromal Heterogeneity and the Ligand-Receptor Interactome by Single-Cell Transcriptomics in Real-world Pancreatic Cancer Biopsies**. *Clin Cancer Res*. 2021;27(21):5912-5921. doi:10.1158/1078-0432.CCR-20-3925

10- Wang Y, Liang Y, Xu H, et al. **Single-cell analysis of pancreatic ductal adenocarcinoma identifies a novel fibroblast subtype associated with poor prognosis but better immunotherapy response**. *Cell Discov*. 2021;7(1):36. Published 2021 May 25. doi:10.1038/s41421-021-00271-4

11- Raghavan S, Winter PS, Navia AW, et al. **Microenvironment drives cell state, plasticity, and drug response in pancreatic cancer**. *Cell*. 2021;184(25):6119-6137.e26. doi:10.1016/j.cell.2021.11.017

12- Wu SZ, Al-Eryani G, Roden DL, et al. **A single-cell and spatially resolved atlas of human breast cancers**. *Nat Genet*. 2021;53(9):1334-1347. doi:10.1038/s41588-021-00911-1

13- Bagaev A, Kotlov N, Nomie K, et al. **Conserved pan-cancer microenvironment subtypes predict response to immunotherapy**. *Cancer Cell*. 2021;39(6):845-865.e7. doi:10.1016/j.ccell.2021.04.014

14- Luca BA, Steen CB, Matusiak M, et al. **Atlas of clinically distinct cell states and ecosystems across human solid tumors**. *Cell*. 2021;184(21):5482-5496.e28. doi:10.1016/j.cell.2021.09.014

15- Storrs EP, Usmani A, Chati P, et al. **High-dimensional deconstruction of pancreatic ductal adenocarcinoma identifies tumor microenvironmental communities associated with survival**. *medRxiv*. 2022; doi:10.1101/2022.04.29.22274376

16- Steele NG, Carpenter ES, Kemp SB, et al. **Multimodal Mapping of the Tumor and Peripheral Blood Immune Landscape in Human Pancreatic Cancer**. *Nat Cancer*. 2020;1(11):1097-1112. doi:10.1038/s43018-020-00121-4

17- Peng J, Sun BF, Chen CY, et al. **Single-cell RNA-seq highlights intra-tumoral heterogeneity and malignant progression in pancreatic ductal adenocarcinoma** [published correction appears in Cell Res. 2019 Aug 13;:]. *Cell Res*. 2019;29(9):725-738. doi:10.1038/s41422-019-0195-y

18- Sun D, Wang J, Han Y, et al. **TISCH: a comprehensive web resource enabling interactive single-cell transcriptome visualization of tumor microenvironment**. *Nucleic Acids Res*. 2021;49(D1):D1420-D1430. doi:10.1093/nar/gkaa1020

19- Stuart T, Butler A, Hoffman P, et al. **Comprehensive Integration of Single-Cell Data**. *Cell*. 2019;177(7):1888-1902.e21. doi:10.1016/j.cell.2019.05.031

20- Korsunsky I, Millard N, Fan J, et al. **Fast, sensitive and accurate integration of single-cell data with Harmony**. *Nat Methods*. 2019;16(12):1289-1296. doi:10.1038/s41592-019-0619-0

21- Qadir F, Sadiq S, & Domínguez-Bendala J. (2019, October 11). **3D Plotting of scRNAseq data using Seurat objects (Version 1.3)**. Zenodo. http://doi.org/10.5281/zenodo.3483177

22- Andreatta M, Carmona SJ. UCell: **Robust and scalable single-cell gene signature scoring**. *Comput Struct Biotechnol J*. 2021;19:3796-3798. Published 2021 Jun 30. doi:10.1016/j.csbj.2021.06.043

23- Yu G, Wang LG, Han Y, He QY. **clusterProfiler: an R package for comparing biological themes among gene clusters**. *OMICS*. 2012;16(5):284-287. doi:10.1089/omi.2011.0118

24- Van den Berge K, Roux de Bézieux H, Street K, et al. **Trajectory-based differential expression analysis for single-cell sequencing data**. *Nat Commun*. 2020;11(1):1201. Published 2020 Mar 5. doi:10.1038/s41467-020-14766-3

25- Jin S, Guerrero-Juarez CF, Zhang L, et al. **Inference and analysis of cell-cell communication using CellChat**. *Nat Commun*. 2021;12(1):1088. Published 2021 Feb 17. doi:10.1038/s41467-021-21246-9

26- Collisson EA, Sadanandam A, Olson P, et al. **Subtypes of pancreatic ductal adenocarcinoma and their differing responses to therapy**. *Nat Med*. 2011;17(4):500-503. doi:10.1038/nm.2344

27- Bailey P, Chang DK, Nones K, et al. **Genomic analyses identify molecular subtypes of pancreatic cancer**. *Nature*. 2016;531(7592):47-52. doi:10.1038/nature16965

28- Mogilenko DA, Shpynov O, Andhey PS, et al. **Comprehensive Profiling of an Aging Immune System Reveals Clonal GZMK+ CD8+ T Cells as Conserved Hallmark of Inflammaging**. *Immunity*. 2021;54(1):99-115.e12. doi:10.1016/j.immuni.2020.11.005

29- Aran D, Camarda R, Odegaard J, et al. **Comprehensive analysis of normal adjacent to tumor transcriptomes**. *Nat Commun*. 2017;8(1):1077. Published 2017 Oct 20. doi:10.1038/s41467-017-01027-z

30- Mathewson ND, Ashenberg O, Tirosh I, et al. **Inhibitory CD161 receptor identified in glioma-infiltrating T cells by single-cell analysis**. *Cell*. 2021;184(5):1281-1298.e26. doi:10.1016/j.cell.2021.01.022

31- Lei Y, Takahama Y. **XCL1 and XCR1 in the immune system**. *Microbes Infect*. 2012;14(3):262-267. doi:10.1016/j.micinf.2011.10.003

32- Böttcher JP, Bonavita E, Chakravarty P, et al. **NK Cells Stimulate Recruitment of cDC1 into the Tumor Microenvironment Promoting Cancer Immune Control**. *Cell*. 2018;172(5):1022-1037.e14. doi:10.1016/j.cell.2018.01.004

33- Kemp SB, Pasca di Magliano M, Crawford HC. **Myeloid Cell Mediated Immune Suppression in Pancreatic Cancer**. *Cell Mol Gastroenterol Hepatol*. 2021;12(5):1531-1542. doi:10.1016/j.jcmgh.2021.07.006

34- Cheng S, Li Z, Gao R, et al. **A pan-cancer single-cell transcriptional atlas of tumor infiltrating myeloid cells**. *Cell*. 2021;184(3):792-809.e23. doi:10.1016/j.cell.2021.01.010

35- Yang L, Zhang Y. **Tumor-associated macrophages: from basic research to clinical application**. *J Hematol Oncol*. 2017;10(1):58. Published 2017 Feb 28. doi:10.1186/s13045-017-0430-2

36- Robinson A, Han CZ, Glass CK, Pollard JW. **Monocyte Regulation in Homeostasis and Malignancy**. *Trends Immunol*. 2021;42(2):104-119. doi:10.1016/j.it.2020.12.001

37- Revel M, Sautès-Fridman C, Fridman WH, Roumenina LT. **C1q+ macrophages: passengers or drivers of cancer progression**. *Trends Cancer*. 2022;8(7):517-526. doi:10.1016/j.trecan.2022.02.006

38- Nalio Ramos R, Missolo-Koussou Y, Gerber-Ferder Y, et al. **Tissue-resident FOLR2+ macrophages associate with CD8+ T cell infiltration in human breast cancer**. *Cell*. 2022;185(7):1189-1207.e25. doi:10.1016/j.cell.2022.02.021

39- Kemp SB, Carpenter ES, Steele NG, et al. **Apolipoprotein E Promotes Immune Suppression in Pancreatic Cancer through NF-κB-Mediated Production of CXCL1**. *Cancer Res*. 2021;81(16):4305-4318. doi:10.1158/0008-5472.CAN-20-3929

40- Hegde S, Krisnawan VE, Herzog BH, et al. **Dendritic Cell Paucity Leads to Dysfunctional Immune Surveillance in Pancreatic Cancer**. *Cancer Cell*. 2020;37(3):289-307.e9. doi:10.1016/j.ccell.2020.02.008

41- Spranger S, Dai D, Horton B, Gajewski TF. **Tumor-Residing Batf3 Dendritic Cells Are Required for Effector T Cell Trafficking and Adoptive T Cell Therapy**. *Cancer Cell*. 2017;31(5):711-723.e4. doi:10.1016/j.ccell.2017.04.003

42- Bosteels C, Neyt K, Vanheerswynghels M, et al. **Inflammatory Type 2 cDCs Acquire Features of cDC1s and Macrophages to Orchestrate Immunity to Respiratory Virus Infection**. *Immunity*. 2020;52(6):1039-1056.e9. doi:10.1016/j.immuni.2020.04.005

43- Zhan HX, Zhou B, Cheng YG, et al. **Crosstalk between stromal cells and cancer cells in pancreatic cancer: New insights into stromal biology**. *Cancer Lett*. 2017;392:83-93. doi:10.1016/j.canlet.2017.01.041

44- Thomas D, Radhakrishnan P. **Tumor-stromal crosstalk in pancreatic cancer and tissue fibrosis**. *Mol Cancer*. 2019;18(1):14. Published 2019 Jan 21. doi:10.1186/s12943-018-0927-5

45- Zhang Y, Crawford HC, Pasca di Magliano M. **Epithelial-Stromal Interactions in Pancreatic Cancer**. *Annu Rev Physiol*. 2019;81:211-233. doi:10.1146/annurev-physiol-020518-114515

46- Bachem MG, Zhou Z, Zhou S, Siech M. **Role of stellate cells in pancreatic fibrogenesis associated with acute and chronic pancreatitis**. *J Gastroenterol Hepatol*. 2006;21 Suppl 3:S92-S96. doi:10.1111/j.1440-1746.2006.04592.x

47- Jin G, Hong W, Guo Y, Bai Y, Chen B. **Molecular Mechanism of Pancreatic Stellate Cells Activation in Chronic Pancreatitis and Pancreatic Cancer**. *J Cancer*. 2020;11(6):1505-1515. Published 2020 Jan 14. doi:10.7150/jca.38616

48- Dobie R, Wilson-Kanamori JR, Henderson BEP, et al. **Single-Cell Transcriptomics Uncovers Zonation of Function in the Mesenchyme during Liver Fibrosis**. *Cell Rep*. 2019;29(7):1832-1847.e8. doi:10.1016/j.celrep.2019.10.024

49- Elyada E, Bolisetty M, Laise P, et al. **Cross-Species Single-Cell Analysis of Pancreatic Ductal Adenocarcinoma Reveals Antigen-Presenting Cancer-Associated Fibroblasts**. *Cancer Discov*. 2019;9(8):1102-1123. doi:10.1158/2159-8290.CD-19-0094

50 - Kinny-Köster B, Guinn S, Tandurella JA, et al. **Inflammatory Signaling and Fibroblast-Cancer Cell Interactions Transfer from a Harmonized Human Single-cell RNA Sequencing Atlas of Pancreatic Ductal Adenocarcinoma to Organoid Co-Culture**. *bioRxiv*. doi:https://doi.org/10.1101/2022.07.14.500096

51- Öhlund D, Handly-Santana A, Biffi G, et al. **Distinct populations of inflammatory fibroblasts and myofibroblasts in pancreatic cancer**. *J Exp Med*. 2017;214(3):579-596. doi:10.1084/jem.20162024

52- Biffi G, Tuveson DA. **Diversity and Biology of Cancer-Associated Fibroblasts**. *Physiol Rev*. 2021;101(1):147-176. doi:10.1152/physrev.00048.2019

53- Sahai E, Astsaturov I, Cukierman E, et al. **A framework for advancing our understanding of cancer-associated fibroblasts**. *Nat Rev Cancer*. 2020;20(3):174-186. doi:10.1038/s41568-019-0238-1

54- Helms EJ, Berry MW, Chaw RC, et al. **Mesenchymal Lineage Heterogeneity Underlies Nonredundant Functions of Pancreatic Cancer-Associated Fibroblasts**. *Cancer Discov*. 2022;12(2):484-501. doi:10.1158/2159-8290.CD-21-0601

55- Biffi G, Oni TE, Spielman B, et al. **IL1-Induced JAK/STAT Signaling Is Antagonized by TGFβ to Shape CAF Heterogeneity in Pancreatic Ductal Adenocarcinoma**. *Cancer Discov*. 2019;9(2):282-301. doi:10.1158/2159-8290.CD-18-0710

56- Steele NG, Biffi G, Kemp SB, et al. **Inhibition of Hedgehog Signaling Alters Fibroblast Composition in Pancreatic Cancer**. *Clin Cancer Res*. 2021;27(7):2023-2037. doi:10.1158/1078-0432.CCR-20-3715

57- Li B, Pei G, Yao J, Ding Q, Jia P, Zhao Z. **Cell-type deconvolution analysis identifies cancer-associated myofibroblast component as a poor prognostic factor in multiple cancer types**. *Oncogene*. 2021;40(28):4686-4694. doi:10.1038/s41388-021-01870-x

58- Ligorio M, Sil S, Malagon-Lopez J, et al. **Stromal Microenvironment Shapes the Intratumoral Architecture of Pancreatic Cancer**. *Cell*. 2019;178(1):160-175.e27. doi:10.1016/j.cell.2019.05.012

59- Lodestijn SC, Miedema DM, Lenos KJ, et al. **Marker-free lineage tracing reveals an environment-instructed clonogenic hierarchy in pancreatic cancer**. *Cell Rep*. 2021;37(3):109852. doi:10.1016/j.celrep.2021.109852

60- Ene-Obong A, Clear AJ, Watt J, et al. **Activated pancreatic stellate cells sequester CD8+ T cells to reduce their infiltration of the juxtatumoral compartment of pancreatic ductal adenocarcinoma**. *Gastroenterology*. 2013;145(5):1121-1132. doi:10.1053/j.gastro.2013.07.025

61- Zhu Y, Knolhoff BL, Meyer MA, et al. **CSF1/CSF1R blockade reprograms tumor-infiltrating macrophages and improves response to T-cell checkpoint immunotherapy in pancreatic cancer models**. *Cancer Res*. 2014;74(18):5057-5069. doi:10.1158/0008-5472.CAN-13-3723

62- Carstens JL, Correa de Sampaio P, Yang D, et al. **Spatial computation of intratumoral T cells correlates with survival of patients with pancreatic cancer**. *Nat Commun*. 2017;8:15095. Published 2017 Apr 27. doi:10.1038/ncomms15095

63- Candido JB, Morton JP, Bailey P, et al. **CSF1R+ Macrophages Sustain Pancreatic Tumor Growth through T Cell Suppression and Maintenance of Key Gene Programs that Define the Squamous Subtype**. *Cell Rep*. 2018;23(5):1448-1460. doi:10.1016/j.celrep.2018.03.131

64- Karamitopoulou E. **Tumour microenvironment of pancreatic cancer: immune landscape is dictated by molecular and histopathological features**. *Br J Cancer*. 2019;121(1):5-14. doi:10.1038/s41416-019-0479-5

65- Winkler J, Abisoye-Ogunniyan A, Metcalf KJ, Werb Z. **Concepts of extracellular matrix remodelling in tumour progression and metastasis**. *Nat Commun*. 2020;11(1):5120. Published 2020 Oct 9. doi:10.1038/s41467-020-18794-x

66- Özdemir BC, Pentcheva-Hoang T, Carstens JL, et al. **Depletion of carcinoma-associated fibroblasts and fibrosis induces immunosuppression and accelerates pancreas cancer with reduced survival** [published correction appears in Cancer Cell. 2015 Dec 14;28(6):831-3]. *Cancer Cell*. 2014;25(6):719-734. doi:10.1016/j.ccr.2014.04.005

67- Chen Y, Kim J, Yang S, et al. **Type I collagen deletion in αSMA+ myofibroblasts augments immune suppression and accelerates progression of pancreatic cancer**. *Cancer Cell*. 2021;39(4):548-565.e6. doi:10.1016/j.ccell.2021.02.007

68- Zhang L, Li Z, Skrzypczynska KM, et al. **Single-Cell Analyses Inform Mechanisms of Myeloid-Targeted Therapies in Colon Cancer**. *Cell*. 2020;181(2):442-459.e29. doi:10.1016/j.cell.2020.03.048

69- Wolf Y, Anderson AC, Kuchroo VK. **TIM3 comes of age as an inhibitory receptor**. *Nat Rev Immunol*. 2020;20(3):173-185. doi:10.1038/s41577-019-0224-6

70- Dixon KO, Tabaka M, Schramm MA, et al. **TIM-3 restrains anti-tumour immunity by regulating inflammasome activation**. *Nature*. 2021;595(7865):101-106. doi:10.1038/s41586-021-03626-9

71- Muthuswamy R, McGray AR, Battaglia S, et al. **CXCR6 by increasing retention of memory CD8+ T cells in the ovarian tumor microenvironment promotes immunosurveillance and control of ovarian cancer**. *J Immunother Cancer*. 2021;9(10):e003329. doi:10.1136/jitc-2021-003329

72- Seo YD, Jiang X, Sullivan KM, et al. **Mobilization of CD8+ T Cells via CXCR4 Blockade Facilitates PD-1 Checkpoint Therapy in Human Pancreatic Cancer**. *Clin Cancer Res*. 2019;25(13):3934-3945. doi:10.1158/1078-0432.CCR-19-0081

73- Chijimatsu R, Kobayashi S, Takeda Y, et al. **Establishment of a reference single-cell RNA sequencing dataset for human pancreatic adenocarcinoma**. *iScience*. 2022;25(8):104659. Published 2022 Jun 22. doi:10.1016/j.isci.2022.104659

74- Werba G, Weissinger D, Kawaler EA, et al. **Single-Cell RNA Sequencing Reveals the Effects of Chemotherapy on Human Pancreatic Adenocarcinoma and its Tumor Microenvironment**. *bioRxiv*. doi:https://doi.org/10.1101/2022.05.24.493132

75- Sautès-Fridman C, Petitprez F, Calderaro J, Fridman WH. **Tertiary lymphoid structures in the era of cancer immunotherapy**. *Nat Rev Cancer*. 2019;19(6):307-325. doi:10.1038/s41568-019-0144-6

76- Kanao H, Enomoto T, Kimura T, et al. **Overexpression of LAMP3/TSC403/DC-LAMP promotes metastasis in uterine cervical cancer**. *Cancer Res*. 2005;65(19):8640-8645. doi:10.1158/0008-5472.CAN-04-4112

77- de Mingo Pulido Á, Gardner A, Hiebler S, et al. **TIM-3 Regulates CD103+ Dendritic Cell Function and Response to Chemotherapy in Breast Cancer**. *Cancer Cell*. 2018;33(1):60-74.e6. doi:10.1016/j.ccell.2017.11.019

78- Nishimura J, Tanaka H, Yamakoshi Y, et al. **Impact of tumor-infiltrating LAMP-3 dendritic cells on the prognosis of esophageal squamous cell carcinoma**. *Esophagus*. 2019;16(4):333-344. doi:10.1007/s10388-019-00669-w

79- Liu Y, He S, Wang XL, et al. **Tumour heterogeneity and intercellular networks of nasopharyngeal carcinoma at single cell resolution**. *Nat Commun*. 2021;12(1):741. Published 2021 Feb 2. doi:10.1038/s41467-021-21043-4

80- Velez-Delgado A, Donahue KL, Brown KL, et al. **Extrinsic KRAS Signaling Shapes the Pancreatic Microenvironment Through Fibroblast Reprogramming**. *Cell Mol Gastroenterol Hepatol*. 2022;13(6):1673-1699. doi:10.1016/j.jcmgh.2022.02.016

81- Fan JQ, Wang MF, Chen HL, Shang D, Das JK, Song J. **Current advances and outlooks in immunotherapy for pancreatic ductal adenocarcinoma**. *Mol Cancer*. 2020;19(1):32. Published 2020 Feb 15. doi:10.1186/s12943-020-01151-3

82- Lesch S, Blumenberg V, Stoiber S, et al. **T cells armed with C-X-C chemokine receptor type 6 enhance adoptive cell therapy for pancreatic tumours**. *Nat Biomed Eng*. 2021;5(11):1246-1260. doi:10.1038/s41551-021-00737-6

83- Nallasamy P, Nimmakayala RK, Karmakar S, et al. **Pancreatic Tumor Microenvironment Factor Promotes Cancer Stemness via SPP1-CD44 Axis**. *Gastroenterology*. 2021;161(6):1998-2013.e7. doi:10.1053/j.gastro.2021.08.023

84- Moncada R, Barkley D, Wagner F, et al. **Integrating microarray-based spatial transcriptomics and single-cell RNA-seq reveals tissue architecture in pancreatic ductal adenocarcinomas** [published correction appears in Nat Biotechnol. 2020 Dec;38(12):1476]. *Nat Biotechnol*. 2020;38(3):333-342. doi:10.1038/s41587-019-0392-8

85- Hwang WL, Jagadeesh KA, Guo JA, et al. **Single-nucleus and spatial transcriptome profiling of pancreatic cancer identifies multicellular dynamics associated with neoadjuvant treatment**. *Nat Genet*. 2022;54(8):1178-1191. doi:10.1038/s41588-022-01134-8

86- Cui Zhou D, Jayasinghe RG, Chen S, et al. **Spatially restricted drivers and transitional cell populations cooperate with the microenvironment in untreated and chemo-resistant pancreatic cancer**. *Nat Genet*. 2022;54(9):1390-1405. doi:10.1038/s41588-022-01157-1

## 7. CONCLUSÕES E PERSPECTIVAS

Nossos resultados trazem uma caracterização refinada da composição e das principais interações celulares do microambiente em diferentes condições biológicas do ADP. Encontramos uma maior proporção de células CD8 de memória nas amostras de tecido adjacente, enquanto as amostras de ADP primário e metastático apresentaram enriquecimento em uma população disfuncional de linfócitos CD8 ($GZMK^+$ CD8). Essa disparidade na distribuição das populações de linfócitos CD8 pode ser explicada pela maior expressão de *CXCR6* no tecido adjacente, mas não podemos descartar a relevância da reação desmoplásica que dificulta os processos de infiltração e migração dos linfócitos no microambiente tendo em vista que observamos enriquecimento de myCAF nas amostras de ADP primário e metastáticas. O enriquecimento de células CD8 de memória no tecido adjacente não é uma particularidade do ADP, pois o mesmo já foi observado em outras neoplasias. Sendo assim, esta diferença na distribuição espacial das células CD8 de memória seria o resultado da reação do hospedeiro ao tumor ou do escape imunológico? Uma possível abordagem para investigar esse aspecto seria a integração de datasets contendo amostras de tecido adjacente e tumor primário de diversas neoplasias. Após a identificação dos clusters, comparar as distribuições e investigar possíveis diferenças epigenéticas entre as populações de linfócitos do tecido adjacente em comparação aos linfócitos do tecido maligno. Outro aspecto relevante seria avaliar a clonalidade desses linfócitos através de dados de scTCR-seq (sequenciamento do receptor de linfócitos T em células individuais), no entanto a disponibilidade desses dados é limitada porque a técnica não é tão popular quanto scRNA-seq.

As células mielóides, especialmente os macrófagos e monócitos, são grandes personagens envolvidos na manutenção do microambiente imunossupressor do ADP. A coexpressão de genes relacionados ao sistema complemento, apresentação de antígeno e resposta ao estresse pela população de macrófagos $APOE^+$ sugere um fenótipo altamente plástico, considerando que essa população pode originar as populações $C1Q^+$ e $SPP1^+$, que por sua vez apresentam funções diferentes. Uma análise isolada da população de macrófagos $APOE^+$ buscando por fatores de transcrição e genes diferencialmente expressos pode contribuir para melhor compreensão dessa heterogeneidade. A presença de células dendríticas $LAMP3^+$ indica a potencial presença de estruturas terciárias linfóides, contudo não podemos afirmar isso na ausência de referência espacial (lâminas de HE ou transcriptômica espacial). A presença dessas estruturas assim como a sua localização no microambiente pode predizer o prognóstico dos pacientes. Um dos nossos objetivos futuros é a elaborar um protocolo para identificação e quantificação das estruturas terciárias linfóides, assim

como explorar a composição do microambiente tumoral nas amostras do Hospital de Clínicas de Porto Alegre (HCPA).

Análises multimodais são cada vez mais frequentes e possibilitam uma visão integrada da heterogeneidade tumoral. Os resultados obtidos aqui servirão como base para análises de deconvolução de bulk RNA-seq permitindo aumentar o ‘n’ amostral, assim como correlacionar a composição do microambiente com a sobrevida dos pacientes. Sabemos que perdemos resolução espacial quando utilizamos scRNA-seq, mas integrando nossos resultados com dados de transcriptômica espacial será possível visualizar a distribuição dos clusters no microambiente e validar a predição das interações celulares. Considerando todo esse contexto do ecossistema tumoral, analisar a composição do microambiente e interações celulares sem levar em conta a distribuição espacial parece pouco representativa da complexidade de um tumor. Sendo assim, a utilização de algoritmos como EcoTyper e DIALOGUE, os quais possibilitam a identificação de ecótipos tumorais em amostras de scRNA-seq e bulk RNA-seq e a identificação de programas multicelulares, respectivamente, será de grande valia.

## REFERÊNCIAS


Almagro J, Messal HA, Elosegui-Artola A, van Rheenen J, Behrens A. **Tissue architecture in tumor initiation and progression**. *Trends Cancer*. 2022;8(6):494-505. doi:10.1016/j.trecan.2022.02.007

Bagaev A, Kotlov N, Nomie K, et al. **Conserved pan-cancer microenvironment subtypes predict response to immunotherapy**. *Cancer Cell*. 2021;39(6):845-865.e7. doi:10.1016/j.ccell.2021.04.014

Balachandran VP, Beatty GL, Dougan SK. **Broadening the Impact of Immunotherapy to Pancreatic Cancer: Challenges and Opportunities**. *Gastroenterology*. 2019;156(7):2056-2072. doi:10.1053/j.gastro.2018.12.038

Barsoum IB, Smallwood CA, Siemens DR, Graham CH. **A mechanism of hypoxia-mediated escape from adaptive immunity in cancer cells**. *Cancer Res*. 2014;74(3):665-674. doi:10.1158/0008-5472.CAN-13-0992

Bell ATF, Mitchell JT, Kiemen AL, et al. **Spatial transcriptomics of FFPE pancreatic intraepithelial neoplasias reveals cellular and molecular alterations of progression to pancreatic ductal carcinoma**. *bioRxiv*. doi:https://doi.org/10.1101/2022.07.16.500312

Biffi G, Tuveson DA. **Diversity and Biology of Cancer-Associated Fibroblasts**. *Physiol Rev*. 2021;101(1):147-176. doi:10.1152/physrev.00048.2019

Carstens JL, Correa de Sampaio P, Yang D, et al. **Spatial computation of intratumoral T cells correlates with survival of patients with pancreatic cancer**. *Nat Commun*. 2017;8:15095. Published 2017 Apr 27. doi:10.1038/ncomms15095

Chan-Seng-Yue M, Kim JC, Wilson GW, et al. **Transcription phenotypes of pancreatic cancer are driven by genomic events during tumor evolution** [published correction appears in Nat Genet. 2020 Feb 12;:]. *Nat Genet*. 2020;52(2):231-240. doi:10.1038/s41588-019-0566-9

Chen Y, Kim J, Yang S, et al. **Type I collagen deletion in αSMA+ myofibroblasts augments immune suppression and accelerates progression of pancreatic cancer**. *Cancer Cell*. 2021;39(4):548-565.e6. doi:10.1016/j.ccell.2021.02.007

Cheng S, Li Z, Gao R, et al. **A pan-cancer single-cell transcriptional atlas of tumor infiltrating myeloid cells**. *Cell*. 2021;184(3):792-809.e23. doi:10.1016/j.cell.2021.01.010

Colligan SH, Tzetzo SL, Abrams SI. **Myeloid-driven mechanisms as barriers to antitumor CD8+ T cell activity**. *Mol Immunol*. 2020;118:165-173. doi:10.1016/j.molimm.2019.12.012

Connor AA, Gallinger S. **Pancreatic cancer evolution and heterogeneity: integrating omics and clinical data**. *Nat Rev Cancer*. 2022;22(3):131-142. doi:10.1038/s41568-021-00418-1

Costa A, Kieffer Y, Scholer-Dahirel A, et al. **Fibroblast Heterogeneity and Immunosuppressive Environment in Human Breast Cancer**. *Cancer Cell*. 2018;33(3):463-479.e10. doi:10.1016/j.ccell.2018.01.011

Crompton T, Outram SV, Hager-Theodorides AL. **Sonic hedgehog signalling in T-cell development and activation**. *Nat Rev Immunol*. 2007;7(9):726-735. doi:10.1038/nri2151

Cui Zhou D, Jayasinghe RG, Chen S, et al. **Spatially restricted drivers and transitional cell populations cooperate with the microenvironment in untreated and chemo-resistant pancreatic cancer**. *Nat Genet*. 2022;54(9):1390-1405. doi:10.1038/s41588-022-01157-1

de la Roche M, Ritter AT, Angus KL, et al. **Hedgehog signaling controls T cell killing at the immunological synapse**. *Science*. 2013;342(6163):1247-1250. doi:10.1126/science.1244689

Delvecchio FR, Fincham REA, Spear S, et al. **Pancreatic Cancer Chemotherapy Is Potentiated by Induction of Tertiary Lymphoid Structures in Mice**. *Cell Mol Gastroenterol Hepatol*. 2021;12(5):1543-1565. doi:10.1016/j.jcmgh.2021.06.023

Dominguez CX, Müller S, Keerthivasan S, et al. **Single-Cell RNA Sequencing Reveals Stromal Evolution into LRRC15+ Myofibroblasts as a Determinant of Patient Response to Cancer Immunotherapy**. *Cancer Discov*. 2020;10(2):232-253. doi:10.1158/2159-8290.CD-19-0644

Dougan SK. **The Pancreatic Cancer Microenvironment**. *Cancer J*. 2017;23(6):321-325. doi:10.1097/PPO.0000000000000288

Elyada E, Bolisetty M, Laise P, et al. **Cross-Species Single-Cell Analysis of Pancreatic Ductal Adenocarcinoma Reveals Antigen-Presenting Cancer-Associated Fibroblasts**. *Cancer Discov*. 2019;9(8):1102-1123. doi:10.1158/2159-8290.CD-19-0094

Ene-Obong A, Clear AJ, Watt J, et al. **Activated pancreatic stellate cells sequester CD8+ T cells to reduce their infiltration of the juxtatumoral compartment of pancreatic ductal adenocarcinoma**. *Gastroenterology*. 2013;145(5):1121-1132. doi:10.1053/j.gastro.2013.07.025

Garg B, Giri B, Modi S, et al. **NFκB in Pancreatic Stellate Cells Reduces Infiltration of Tumors by Cytotoxic T Cells and Killing of Cancer Cells, via Up-regulation of CXCL12**. *Gastroenterology*. 2018;155(3):880-891.e8. doi:10.1053/j.gastro.2018.05.051

Grünwald BT, Devisme A, Andrieux G, et al. **Spatially confined sub-tumor microenvironments in pancreatic cancer**. *Cell*. 2021;184(22):5577-5592.e18. doi:10.1016/j.cell.2021.09.022

Haeberle L, Esposito I. **Pathology of pancreatic cancer**. *Transl Gastroenterol Hepatol*. 2019;4:50. Published 2019 Jun 27. doi:10.21037/tgh.2019.06.02

Hayashi A, Fan J, Chen R, et al. **A unifying paradigm for transcriptional heterogeneity and squamous features in pancreatic ductal adenocarcinoma**. *Nat Cancer*. 2020;1(1):59-74. doi:10.1038/s43018-019-0010-1

Hayashi A, Hong J, Iacobuzio-Donahue CA. **The pancreatic cancer genome revisited**. *Nat Rev Gastroenterol Hepatol*. 2021;18(7):469-481. doi:10.1038/s41575-021-00463-z

Hegde S, Krisnawan VE, Herzog BH, et al. **Dendritic Cell Paucity Leads to Dysfunctional Immune Surveillance in Pancreatic Cancer**. *Cancer Cell*. 2020;37(3):289-307.e9. doi:10.1016/j.ccell.2020.02.008

Helms EJ, Berry MW, Chaw RC, et al. **Mesenchymal Lineage Heterogeneity Underlies Nonredundant Functions of Pancreatic Cancer-Associated Fibroblasts**. *Cancer Discov*. 2022;12(2):484-501. doi:10.1158/2159-8290.CD-21-0601

Hessmann E, Patzak MS, Klein L, et al. **Fibroblast drug scavenging increases intratumoural gemcitabine accumulation in murine pancreas cancer**. *Gut*. 2018;67(3):497-507. doi:10.1136/gutjnl-2016-311954

Hiraoka N, Ino Y, Yamazaki-Itoh R, Kanai Y, Kosuge T, Shimada K. **Intratumoral tertiary lymphoid organ is a favourable prognosticator in patients with pancreatic cancer**. *Br J Cancer*. 2015;112(11):1782-1790. doi:10.1038/bjc.2015.145

Ho WJ, Jaffee EM, Zheng L. **The tumour microenvironment in pancreatic cancer - clinical challenges and opportunities**. *Nat Rev Clin Oncol*. 2020;17(9):527-540. doi:10.1038/s41571-020-0363-5

Hosein AN, Brekken RA, Maitra A. **Pancreatic cancer stroma: an update on therapeutic targeting strategies**. *Nat Rev Gastroenterol Hepatol*. 2020;17(8):487-505. doi:10.1038/s41575-020-0300-1

Hosein AN, Huang H, Wang Z, et al. **Cellular heterogeneity during mouse pancreatic ductal adenocarcinoma progression at single-cell resolution**. *JCI Insight*. 2019;5(16):e129212. Published 2019 Jul 23. doi:10.1172/jci.insight.129212

Huang H, Wang Z, Zhang Y, et al. **Mesothelial cell-derived antigen-presenting cancer-associated fibroblasts induce expansion of regulatory T cells in pancreatic cancer**. *Cancer Cell*. 2022;40(6):656-673.e7. doi:10.1016/j.ccell.2022.04.011

Jin G, Hong W, Guo Y, Bai Y, Chen B. **Molecular Mechanism of Pancreatic Stellate Cells Activation in Chronic Pancreatitis and Pancreatic Cancer**. *J Cancer*. 2020;11(6):1505-1515. Published 2020 Jan 14. doi:10.7150/jca.38616

Kanda M, Matthaei H, Wu J, et al. **Presence of somatic mutations in most early-stage pancreatic intraepithelial neoplasia**. *Gastroenterology*. 2012;142(4):730-733.e9. doi:10.1053/j.gastro.2011.12.042

Karamitopoulou E. **Tumour microenvironment of pancreatic cancer: immune landscape is dictated by molecular and histopathological features**. *Br J Cancer*. 2019;121(1):5-14. doi:10.1038/s41416-019-0479-5

Kemp SB, Pasca di Magliano M, Crawford HC. **Myeloid Cell Mediated Immune Suppression in Pancreatic Cancer**. *Cell Mol Gastroenterol Hepatol*. 2021;12(5):1531-1542. doi:10.1016/j.jcmgh.2021.07.006

Kenkel JA, Tseng WW, Davidson MG, et al. **An Immunosuppressive Dendritic Cell Subset Accumulates at Secondary Sites and Promotes Metastasis in Pancreatic Cancer**. *Cancer Res*. 2017;77(15):4158-4170. doi:10.1158/0008-5472.CAN-16-2212

Kleeff J, Korc M, Apte M, et al. **Pancreatic cancer**. *Nat Rev Dis Primers*. 2016;2:16022. Published 2016 Apr 21. doi:10.1038/nrdp.2016.22

Kurachi M. **CD8+ T cell exhaustion**. *Semin Immunopathol*. 2019;41(3):327-337. doi:10.1007/s00281-019-00744-5

Laklai H, Miroshnikova YA, Pickup MW, et al. **Genotype tunes pancreatic ductal adenocarcinoma tissue tension to induce matricellular fibrosis and tumor progression**. *Nat Med*. 2016;22(5):497-505. doi:10.1038/nm.4082

Lawlor RT, Mattiolo P, Mafficini A, et al. **Tumor Mutational Burden as a Potential Biomarker for Immunotherapy in Pancreatic Cancer: Systematic Review and Still-Open Questions**. *Cancers (Basel)*. 2021;13(13):3119. Published 2021 Jun 22. doi:10.3390/cancers13133119

Ligorio M, Sil S, Malagon-Lopez J, et al. **Stromal Microenvironment Shapes the Intratumoral Architecture of Pancreatic Cancer**. *Cell*. 2019;178(1):160-175.e27. doi:10.1016/j.cell.2019.05.012
Luca BA, Steen CB, Matusiak M, et al. **Atlas of clinically distinct cell states and ecosystems across human solid tumors**. *Cell*. 2021;184(21):5482-5496.e28. doi:10.1016/j.cell.2021.09.014

Luu AM, Belyaev O, Höhn P, et al. **Late recurrences of pancreatic cancer in patients with long-term survival after pancreaticoduodenectomy**. *J Gastrointest Oncol*. 2021;12(2):474-483. doi:10.21037/jgo-20-433

Makohon-Moore AP, Matsukuma K, Zhang M, et al. **Precancerous neoplastic cells can move through the pancreatic ductal system**. *Nature*. 2018;561(7722):201-205. doi:10.1038/s41586-018-0481-8

Makohon-Moore AP, Zhang M, Reiter JG, et al. **Limited heterogeneity of known driver gene mutations among the metastases of individual patients with pancreatic cancer**. Nat Genet. 2017;49(3):358-366. doi:10.1038/ng.3764

Nagathihalli NS, Castellanos JA, Shi C, et al. **Signal Transducer and Activator of Transcription 3, Mediated Remodeling of the Tumor Microenvironment Results in Enhanced Tumor Drug Delivery in a Mouse Model of Pancreatic Cancer**. *Gastroenterology*. 2015;149(7):1932-1943.e9. doi:10.1053/j.gastro.2015.07.058

Notta F, Chan-Seng-Yue M, Lemire M, et al. **A renewed model of pancreatic cancer evolution based on genomic rearrangement patterns** [published correction appears in Nature. 2017 Feb 2;542(7639):124]. *Nature*. 2016;538(7625):378-382. doi:10.1038/nature19823

Ogawa Y, Masugi Y, Abe T, et al. **Three Distinct Stroma Types in Human Pancreatic Cancer Identified by Image Analysis of Fibroblast Subpopulations and Collagen**. *Clin Cancer Res*. 2021;27(1):107-119. doi:10.1158/1078-0432.CCR-20-2298

Öhlund D, Franklin O, Lundberg E, Lundin C, Sund M. **Type IV collagen stimulates pancreatic cancer cell proliferation, migration, and inhibits apoptosis through an autocrine loop**. *BMC Cancer*. 2013;13:154. Published 2013 Mar 26. doi:10.1186/1471-2407-13-154

Öhlund D, Handly-Santana A, Biffi G, et al. **Distinct populations of inflammatory fibroblasts and myofibroblasts in pancreatic cancer**. *J Exp Med*. 2017;214(3):579-596. doi:10.1084/jem.20162024

Ohm JE, Gabrilovich DI, Sempowski GD, et al. **VEGF inhibits T-cell development and may contribute to tumor-induced immune suppression**. *Blood*. 2003;101(12):4878-4886. doi:10.1182/blood-2002-07-1956

Özdemir BC, Pentcheva-Hoang T, Carstens JL, et al. **Depletion of carcinoma-associated fibroblasts and fibrosis induces immunosuppression and accelerates pancreas cancer with reduced survival** [published correction appears in Cancer Cell. 2015 Dec 14;28(6):831-3]. *Cancer Cell*. 2014;25(6):719-734. doi:10.1016/j.ccr.2014.04.005

Park W, Chawla A, O'Reilly EM. **Pancreatic Cancer: A Review** [published correction appears in JAMA. 2021 Nov 23;326(20):2081]. *JAMA*. 2021;326(9):851-862. doi:10.1001/jama.2021.13027

Raggi F, Pelassa S, Pierobon D, et al. **Regulation of Human Macrophage M1-M2 Polarization Balance by Hypoxia and the Triggering Receptor Expressed on Myeloid Cells-1**. *Front Immunol*. 2017;8:1097. Published 2017 Sep 7. doi:10.3389/fimmu.2017.01097

Raghavan S, Winter PS, Navia AW, et al. **Microenvironment drives cell state, plasticity, and drug response in pancreatic cancer**. *Cell*. 2021;184(25):6119-6137.e26. doi:10.1016/j.cell.2021.11.017

Rahib L, Smith BD, Aizenberg R, Rosenzweig AB, Fleshman JM, Matrisian LM. **Projecting cancer incidence and deaths to 2030: the unexpected burden of thyroid, liver, and pancreas cancers in the United States** [published correction appears in Cancer Res. 2014 Jul 15;74(14):4006]. *Cancer Res*. 2014;74(11):2913-2921. doi:10.1158/0008-5472.CAN-14-0155

Ramanathan RK, McDonough SL, Philip PA, et al. **Phase IB/II Randomized Study of FOLFIRINOX Plus Pegylated Recombinant Human Hyaluronidase Versus FOLFIRINOX Alone in Patients With Metastatic Pancreatic Adenocarcinoma: SWOG S1313**. *J Clin Oncol*. 2019;37(13):1062-1069. doi:10.1200/JCO.18.01295

Regine WF, Winter KA, Abrams RA, et al. **Fluorouracil vs gemcitabine chemotherapy before and after fluorouracil-based chemoradiation following resection of pancreatic adenocarcinoma: a randomized controlled trial** [published correction appears in JAMA. 2008 Apr 23/30;299(16):1902]. *JAMA*. 2008;299(9):1019-1026. doi:10.1001/jama.299.9.1019

Roth S, Zamzow K, Gaida MM, et al. **Evolution of the immune landscape during progression of pancreatic intraductal papillary mucinous neoplasms to invasive cancer**. *EBioMedicine*. 2020;54:102714. doi:10.1016/j.ebiom.2020.102714

Sahai E, Astsaturov I, Cukierman E, et al. **A framework for advancing our understanding of cancer-associated fibroblasts**. *Nat Rev Cancer*. 2020;20(3):174-186. doi:10.1038/s41568-019-0238-1

Schalck A, Sakellariou-Thompson D, Forget MA, et al. **Single-Cell Sequencing Reveals Trajectory of Tumor-Infiltrating Lymphocyte States in Pancreatic Cancer**. *Cancer Discov*. 2022;12(10):2330-2349. doi:10.1158/2159-8290.CD-21-1248

Schlesinger Y, Yosefov-Levi O, Kolodkin-Gal D, et al. **Single-cell transcriptomes of pancreatic preinvasive lesions and cancer reveal acinar metaplastic cells' heterogeneity**. *Nat Commun*. 2020;11(1):4516. Published 2020 Sep 9. doi:10.1038/s41467-020-18207-z

Siegel RL, Miller KD, Fuchs HE, Jemal A. **Cancer Statistics, 2021** [published correction appears in CA Cancer J Clin. 2021 Jul;71(4):359]. *CA Cancer J Clin*. 2021;71(1):7-33. doi:10.3322/caac.21654

Sohal DPS, Duong M, Ahmad SA, et al. **Efficacy of Perioperative Chemotherapy for Resectable Pancreatic Adenocarcinoma: A Phase 2 Randomized Clinical Trial** [published correction appears in JAMA Oncol. 2021 Sep 23;:null]. *JAMA Oncol*. 2021;7(3):421-427. doi:10.1001/jamaoncol.2020.7328

Steele NG, Biffi G, Kemp SB, et al. **Inhibition of Hedgehog Signaling Alters Fibroblast Composition in Pancreatic Cancer**. *Clin Cancer Res*. 2021;27(7):2023-2037. doi:10.1158/1078-0432.CCR-20-3715

Su S, Chen J, Yao H, et al. **CD10+GPR77+ Cancer-Associated Fibroblasts Promote Cancer Formation and Chemoresistance by Sustaining Cancer Stemness**. *Cell*. 2018;172(4):841-856.e16. doi:10.1016/j.cell.2018.01.009

Sung H, Ferlay J, Siegel RL, et al. Global Cancer Statistics 2020: **GLOBOCAN Estimates of Incidence and Mortality Worldwide for 36 Cancers in 185 Countries**. *CA Cancer J Clin*. 2021;71(3):209-249. doi:10.3322/caac.21660

Togashi Y, Shitara K, Nishikawa H. **Regulatory T cells in cancer immunosuppression - implications for anticancer therapy**. *Nat Rev Clin Oncol*. 2019;16(6):356-371. doi:10.1038/s41571-019-0175-7

Van Cutsem E, Tempero MA, Sigal D, et al. **Randomized Phase III Trial of Pegvorhyaluronidase Alfa With Nab-Paclitaxel Plus Gemcitabine for Patients With Hyaluronan-High Metastatic Pancreatic Adenocarcinoma**. *J Clin Oncol*. 2020;38(27):3185-3194. doi:10.1200/JCO.20.00590

Wei L, Ye H, Li G, et al. **Cancer-associated fibroblasts promote progression and gemcitabine resistance via the SDF-1/SATB-1 pathway in pancreatic cancer** [published correction appears in Cell Death Dis. 2021 Mar 3;12(3):232]. *Cell Death Dis*. 2018;9(11):1065. Published 2018 Oct 18. doi:10.1038/s41419-018-1104-x

Whatcott CJ, Diep CH, Jiang P, et al. **Desmoplasia in Primary Tumors and Metastatic Lesions of Pancreatic Cancer**. *Clin Cancer Res*. 2015;21(15):3561-3568. doi:10.1158/1078-0432.CCR-14-1051

Wherry EJ, Kurachi M. **Molecular and cellular insights into T cell exhaustion**. *Nat Rev Immunol*. 2015;15(8):486-499. doi:10.1038/nri3862

Wu SZ, Al-Eryani G, Roden DL, et al. **A single-cell and spatially resolved atlas of human breast cancers**. *Nat Genet*. 2021;53(9):1334-1347. doi:10.1038/s41588-021-00911-1

Yang S, Liu Q, Liao Q. **Tumor-Associated Macrophages in Pancreatic Ductal Adenocarcinoma: Origin, Polarization, Function, and Reprogramming**. *Front Cell Dev Biol*. 2021;8:607209. Published 2021 Jan 11. doi:10.3389/fcell.2020.607209

Zandberg DP, Menk AV, Velez M, et al. **Tumor hypoxia is associated with resistance to PD-1 blockade in squamous cell carcinoma of the head and neck**. *J Immunother Cancer*. 2021;9(5):e002088. doi:10.1136/jitc-2020-002088

Zhang Y, Kirane A, Huang H, et al. **Cyclooxygenase-2 Inhibition Potentiates the Efficacy of Vascular Endothelial Growth Factor Blockade and Promotes an Immune Stimulatory Microenvironment in Preclinical Models of Pancreatic Cancer**. *Mol Cancer Res*. 2019;17(2):348-355. doi:10.1158/1541-7786.MCR-18-0427